UNIVERSITÀ DEGLI STUDI DI PARMA

DOTTORATO DI RICERCA IN MEDICINA MOLECOLARE

XXIX CICLO

Hyperhydrophilic Implant Titanium Surfaces: Development, Characterization and *in Vitro* Evaluation.

Coordinatore:

Prof. Luciano POLONELLI

Tutor:

Prof. Guido Maria MACALUSO

Dottorando:

Dr. Andrea TOFFOLI

DIPARTIMENTO DI SCIENZE BIOLOGICHE,
BIOTECNOLOGICHE E TRASLAZIONALI

December 12, 2016

"Esistono soltanto due cose: scienza ed opinione; la prima genera conoscenza, la seconda ignoranza."

Ippocrate

UNIVERSITÀ DEGLI STUDI DI PARMA

Abstract

Dottorato di Ricerca in Medicina Molecolare
Dipartimento di Scienze Biologiche, Biotecnologiche e Traslazionali

Doctor of Philosophy

Hyperhydrophilic Implant Titanium Surfaces: Development, Characterization and *in Vitro* Evaluation.

by Dr. Andrea TOFFOLI

In the last years, many authors focused their research on titanium surfaces and on the development of new methods to enhance dental implants properties, seeking for a faster and higher bone apposition. Surface hydrophilicity is a key-feature among the ones affecting dental implants success. In this thesis, we developed a new method to strongly enhance surfaces hydrophilcity, effective both for machined and moderately rough titanium. We analyzed the physico-chemical modifications occured on the surfaces after the treatment, and then we studied bone cells behaviour on treated surfaces in terms of adhesion, proliferation and morphology. Results support the effectiveness of our treatment, which was found to enhance surface protein adsorption and bone cells adhesion on the surfaces while leaving the surface chemical composition almost unmodified, and open to the possibility of testing its effectiveness *in vivo*.

Acknowledgements

The realization of this work would not have been possible without the contribution of some people to which a great acknowledgement belongs:

- My supervisor, Prof. Guido Maria Macaluso, for his precious help and vision;
- The Director of Centro Universitario di Odontoiatria, Prof. Mauro Bonanini;
- Prof. Carlo Galli for his careful guidance;
- Dr. Ludovica Parisi for her essential help with laboratory procedure, data analysis and discussion;
- Prof. Simone Lumetti, Prof. Edoardo Manfredi, and Dr. Federico Rivara for their helpful advices;
- Prof. Ovidio Bussolati and Dr. Massimiliano Bianchi for the realization of SDS-PAGE and Western-Blot analysis;
- Dr. Paola Lagonegro, for SEM-FIB analysis;
- Dr. Roberta Tatti, for XPS analysis;
- Dr. Andrea Lorenzi and Dr. Ilaria Alfieri for Raman Spectroscopy;
- Dr. Francesco Salati and Dr. Beatrice Spaggiari for their inspiring clinical practice;
- Mrs. Stefania Boldrocchi, Mrs. Alessandra Moruzzi, Mrs. Chiara Molinari Tosatti, Dr. Gallia Graiani and Dr. Arianna Smerieri for their costant presence and support.

Contents

Abstract **ii**

Acknowledgements **iii**

I Introduction 1

1 Surface Hydrophilicity of Dental Implants **2**

1.1 Introduction 2

1.1.1 Osseointegration 2

1.1.2 The role of wettability in osseointegration 5

1.2 Biological effectiveness of hyperhydrophilic surfaces . 10

1.2.1 Surface conditioning 10

1.2.2 Cells - surface interaction 11

1.2.3 Osseointegration 12

1.2.4 Bacterial adhesion 15

1.3 Titanium biological aging 18

Bibliography 21

2 Aims **29**

II Experiments 31

3 Machined and ZirTi® surfaces characterization and murine MC3T3-E1 cells biological response **32**

3.1 Introduction 32

3.2 Materials and methods 34
3.2.1 Titanium discs 34
3.2.2 Discs characterization 34
3.2.3 Protein adsorption 35
3.2.4 Cell culture 36
3.2.5 Cell viability 36
3.2.6 Cell metabolic activity 36
3.2.7 Cell morphology 37
3.2.8 Real time PCR 38
3.2.9 Statistical analysis 38
3.3 Results 39
3.3.1 Surface characteristics 39
3.3.2 Protein adsorption 41
3.3.3 Cell proliferation 43
3.3.4 Cell distribution and organization during the adhesion 45
3.3.5 Cell differentiation 45
3.4 Discussion 49
Bibliography 52

4 Surfaces characterization **54**
4.1 Introduction 54
4.2 Materials and methods 57
4.2.1 Titanium discs 57
4.2.2 Surface treatment 57
4.2.3 Physical characterization 58
4.2.4 Chemical characterization 59
4.2.5 Morphology 61
4.2.6 Protein adsorption 61

4.2.7 Statistical analysis 63
4.3 Results 64
4.3.1 Titanium physical properties 64
4.3.2 Titanium chemical properties 67
4.3.3 Titanium morphological properties 74
4.3.4 Protein adsorption 75
4.4 Discussion 82
Bibliography 86

5 Investigation of MC3T3-E1 cells behaviour on the surfaces 89
5.1 Introduction 89
5.2 Materials and methods 91
5.2.1 *In vitro* assays 91
5.2.2 Statistical analysis 95
5.3 Results 96
5.3.1 Cell viability and proliferation 96
5.3.2 Cell adhesion and morphology 100
5.4 Discussion 106
Bibliography 109

6 Conclusions and future perspectives 112
6.1 Conclusions 112
6.2 Future perspectives 114

List of Figures

1.1 Anatomic structures of a tooth and of an implant-supported crown . . . 3
1.2 Gradual shift from implant mechanical stability and implant biological stability . . . 5
1.3 Schematic representation of photocatalysis on titanium dioxide . . . 7
1.4 Effects on cellular adhesion of hydrophobic and hydrophilic surfaces . . . 12

3.1 Typical SEM images of machined and ZirTi® surfaces microtopography . . . 39
3.2 Chemical composition of machined and ZirTi® surfaces analyzed through XPS . . . 39
3.3 Standardized photograph of machined and ZirTi® surfaces wettability measurement . . . 40
3.4 Histogram showing contact angle measurement on machined and ZirTi® surfaces . . . 40
3.5 Amount of protein adsorbed on machined and ZirTi® surfaces . . . 41
3.6 SDS-PAGE of protein adsorbed on machined and ZirTi® surfaces . . . 42
3.7 Histograms showing cell proliferation on machined and ZirTi® surfaces measured through Resazurine Sodium Salt assay . . . 43

3.8 Histogram and relative images showing cell proliferation on machined and ZirTi® surfaces 44
3.9 Typical fluorescence and SEM images showing MC3T3-E1 cells on machined and ZirTi® surfaces 46
3.10 7 days Real Time-PCR results 47
3.11 14 days Real Time-PCR results 48

4.1 Different levels of surface wettability measured through the contact angle of a water droplet 58
4.2 Standardized photograph of a control machined surface showing the contact angle with a drop of water . . 64
4.3 Standardized photograph of a treated machined surface showing the contact angle with a drop of water . . 65
4.4 Standardized photograph of a control ZirTi® surface showing the contact angle with a drop of water 65
4.5 Standardized photograph of a treated ZirTi® surface showing the contact angle with a drop of water 66
4.6 Contact angle measurement on treated and control surfaces 66
4.7 XPS wide range spectrum of the machined and ZirTi® samples 67
4.8 Atomic percentage of all the chemical species present in the samples 68
4.9 XPS core level spectra 69
4.10 Analysis of O1s core level of all the samples 70
4.11 Analysis of Ti2p core level of all the samples 71
4.12 Atomic percentage of the TiO2 and Ti2O3 species in the samples 72
4.13 Raman spectra of ZirTi® surfaces 73

4.14 Raman spectra of machined surfaces 73
4.15 SEM images of surfaces 74
4.16 Curves representing albumine adsorption on machined titanium surfaces over time 75
4.17 Curves representing fibronectin adsorption on machined titanium surfaces over time 76
4.18 Curves representing albumine adsorption on ZirTi® titanium surfaces over time 76
4.19 Curves representing fibronectin adsorption on ZirTi® titanium surfaces over time 77
4.20 SDS-PAGE of protein adsorbed on machined and ZirTi® titanium surfaces 79
4.21 Western Blot analysis of fibrinogen adsorption on machined and ZirTi® titanium surfaces 79
4.22 Western Blot analysis of fibronectin adsorption on machined and ZirTi® titanium surfaces 80
4.23 Western Blot analysis of transferrin adsorption on machined and ZirTi® titanium surfaces 80
4.24 Western Blot analysis of albumin adsorption on machined and ZirTi® titanium surfaces 81

5.1 Diagram representing the method used to design the adhesion trend line of cells to hydrophobic and hydrophilic surfaces 93
5.2 Hydrophilicity influence cell viability on titanium . . . 97
5.3 Histograms showing the mean of viable and dead cells on machined surfaces 98
5.4 Histograms showing the mean of viable and dead cells on ZirTi® surfaces 98

5.5 Histograms showing MC3T3-E1 cells metabolic activity assessed through the Resazurin Sodium salt assay on machined titanium surfaces 24, 48 and 72 hours after seeding 99
5.6 Histograms showing MC3T3-E1 cells metabolic activity assessed through the Resazurin Sodium salt assay on ZirTi® titanium surfaces 24, 48 and 72 hours after seeding 99
5.7 Evolution curves representing MC3T3-E1 cells speed of adhesion to machined surfaces 100
5.8 Evolution curves representing MC3T3-E1 cells speed of adhesion to ZirTi® titanium surfaces 101
5.9 Typical SEM and FIB images of MC3T3-E1 cells cultured on hydrophilic and hydrophobic machined or ZirTi® titanium surfaces after 24 hours of culture 103
5.10 Microphotographs showing MC3T3-E1 cells on hydrophobic and hydrophilic machined titanium surfaces and on hydrophobic and hydrophilic after actin, vinculin and DAPI staining 104
5.11 Histogram showing the average of focal adhesion detected for cell on machined surfaces 105
5.12 Histogram showing the average of focal adhesion detected for cell on ZirTi® surfaces 105

Alla mia famiglia.

Part I

Introduction

Chapter 1

Surface Hydrophilicity of Dental Implants

1.1 Introduction

Dental implants are medical devices inserted in the bone of the oral cavity as dental root replacement (fig.1.1). Many years of interdisciplinary research in the field of dental biomaterials have demonstrated that titanium dental implants are a safe and effective therapeutic option in dentistry. After recognizing that titanium can establish an intimate and direct interaction with bone, termed osseointegration, the metal and its alloys have been used for more than 40 years in the partly or full edentulous mandible and maxilla, for the anchorage of prostheses, crowns or bridges [1].

1.1.1 Osseointegration

Osseointegration, as defined by Branemark and colleagues, is a direct structural and functional connection of a load-carrying implant and consists of direct histological bone-to-implant contact, without an intervening layer of fibrous tissue [2, 3]. Osseointegration results

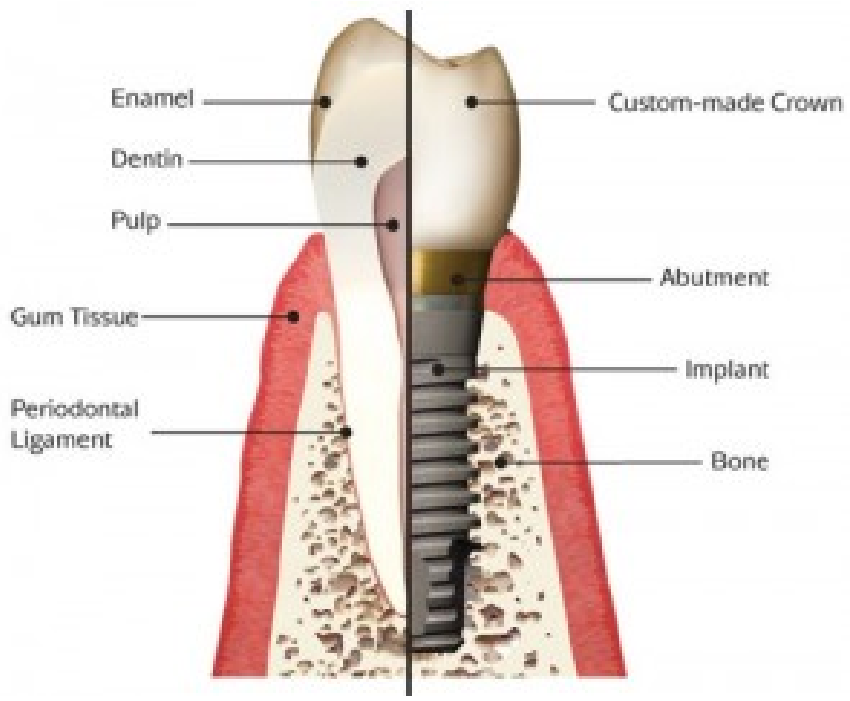

FIGURE 1.1: Anatomic structures of a tooth (left) and of an implant supported crown (right).

from a complex series of molecular processes ultimately leading to the formation of a functional bone-implant interface. Clinically, the first outcome of implant placement surgical procedure is the primary stability of the implant which is a rigid fixation and lack of micro motion of the implant into the bone cavity Absence of stability can lead to excessive mobility and cause fibrous tissue formation around the implants inhibiting osseointegration. Primary stability depends on the surgical technique, implant design and bone quality at the implant site [3, 4, 5].

At a microscopic level, osseointegration begins with bleeding, induced by the osteotomy preparation surgical trauma. When blood comes in contact with the implant surface, triggers a cascade of biological events leading to protein adsorption and coagulation. The blood clot, thus formed, serves as a mechanical scaffold and provides the biochemical components for osteoconduction [6].

Osteoconduction, as described by Davies, consists in the recruitment and migration of osteogenic cells. In particular, mesenchymal stem cells migrate through the preliminary matrix of the fibrin clot toward the implant surface; subsequently, as these cells reach implant surface, signaling molecules and relased transcription factors cause their differentiation into osteoblasts, which are cells able to depose new bone tissue. The starting point of the new bone forming is called distance osteogenesis (DO), while the limit of new bone formed is termed contact osteogenesis (CO) [6].
As healing proceeds, bone formed through DO and CO grows and unifies. Immature bone formed through osteogenesis results in a gradual increase for the secondary stability of the implant. At the same time, remodeling and osteoclastic resorption of bone that was initially in direct contact with the implant, causes a decline in primary stability [7]. The immature bone eventually mineralizes, matures and remodels (fig.1.2).

Albrektsson et al. [8] summarized the factors affecting osseointegration, that include:

- Biocompatibility of the implant material;
- The quality of the bone at the implant site;
- Macro- and microscopic nature of the implant design;
- Dental implant surface properties;
- Undisturbed healing phase.

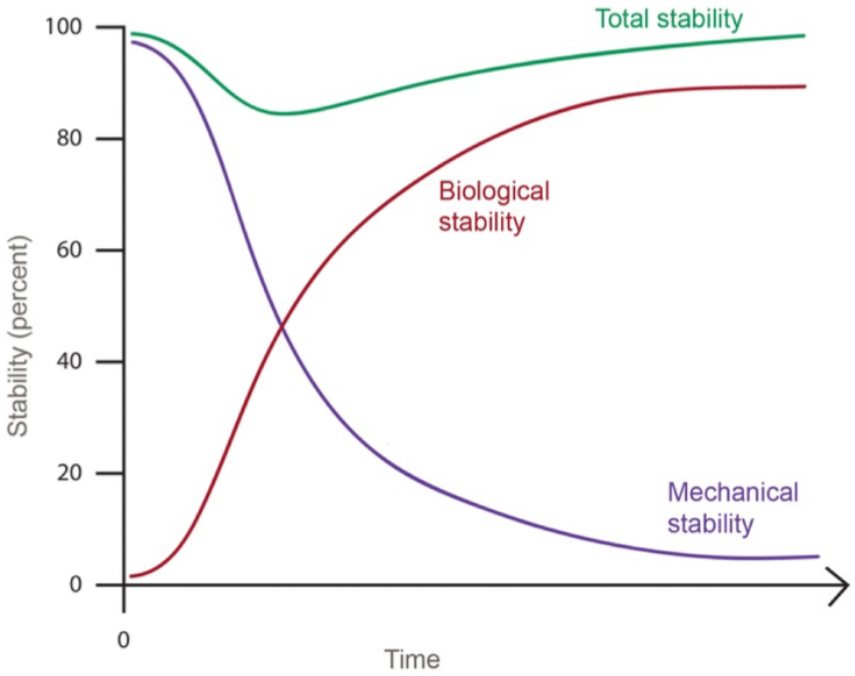

FIGURE 1.2: Gradual shift from implant mechanical stability (primary) and implant biological stability (secondary).

1.1.2 The role of wettability in osseointegration

Among the dental implant properties, surface topography has been considered for years the most important factor, which influences osseointegration and rough implant surfaces have been considered the most suitable option to induce and a fast and more predictable bone formation[9].

In recent years, it has been demonstrated that the surface energy of an implant, measured indirectly by the liquid–solid contact angle (CA) and thus related to wettability, is another important surface characteristic known to affect the biological response to the implant [10, 11]. Many studies have found that hydrophilic surfaces tend to enhance the early stages of cell adhesion, proliferation, differentiation and bone mineralization compared to hydrophobic surface[12, 13]. As just mentioned, in the recent past, surface hydrophilcity was

not considered as a primary feature of dental implants but nowadays many authors have become aware about the importance of implant surfaces wettability and many studies have been published on experimental dental implant surfaces with high hydrophilicity[14, 15] and on wetting-behaviour of commercialy available dental implants[16, 17].

Many factors are known to influence surface wettability. First of all, surface energy of titanium is determined by the surface-charge density and the net polarity of charge. Surfaces positive or negative charge-polarized are capable of bonding hydrogen, presenting higher hydrophilicity if compared to electrically neutral surfaces [18, 19]. It has also been demonstrated that microstructured dental implant surfaces tend to show lower hydrophilicity [16, 17]. Furthermore, the natural-occurring hydrocarbon deposition on surfaces causes a major loss of hydrophilicity [20]. In particular, this phenomenon has been described as 'Biological Aging of Titanium' [21] and it has been identified as the primary cause of time-dependent loss of wetting performances of dental implant. This topic will be fully addressed in the last section of this chapter (page 18). Considering the above mentioned statements, it is evident that the hydrophilicity of a surface could be improved, and in literature several examples are reported.

Photocatalysis

Some authors have used a well-known and commonly used in many fields chemical reaction called photocatalysis to enhance titanium surface hydrophilicity. A photocatalytic reaction consists in the acceleration of a photoreaction through a source of light in the presence of a catalyst. In photogenerated catalysis, the photocatalytic

activity depends on the ability of the catalyst to create electron–hole pairs, which generate free radicals (e.g. hydroxyl radicals: •OH) able to undergo secondary reactions. A photocatalyst is a semiconductor that, by absorbing a photon of energy higher than the gap between the valence band and the conduction band, changes the structure of its molecular orbitals with electrons (called photoelectrons) which go from the valence band to the conduction band, generating positive electron-holes in the valence band (fig.1.3) [22].

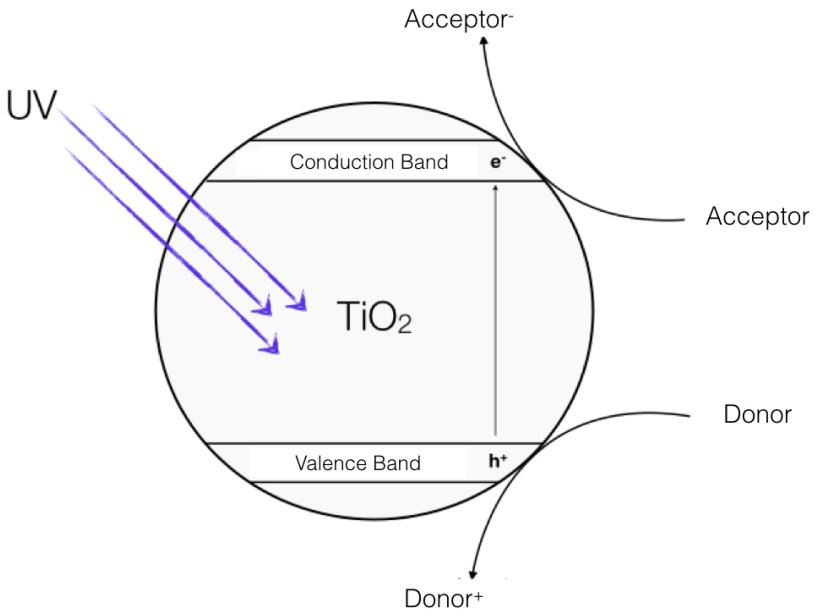

FIGURE 1.3: Schematic representation of photocatalysis on titanium dioxide

There are different hypothesis on how a photocatalytic reaction on titanium surfaces can enhance their wettability[23, 24]:

- the increase of hydrophilicity is directly due to the formation of free radicals on the surface, which easily bind with water;

- the photocatalytic reaction and the free radicals created by the reaction itself destroy hydrocarbons and other organic contaminants present on the surface, making it more suitable to interface with water molecules;

- the photocatalytic reaction generates surface vacancies at bridging sites.

However, photocatalysis (also called "photoactivation") of implant titanium surfaces have to be performed chair-side right before surgical implant placement because its effect are not free from the issue of biological aging of titanium [20, 21, 23].

Gamma-ray treatment

Alternatively, to overcome the issue of titanium biological aging, Ueno and colleagues tested the hypothesis that gamma ray treatment, owing to its high energy to decompose and remove organic contaminants, enhances the bioactivity and osteoconductivity of titanium [25]. In their study titanium disks were acid-etched and stored for 4 weeks. Rat bone marrow–derived osteoblasts (BMOs) were cultured on titanium disks with or without gamma ray treatment (30 kGy) immediately before experiments. Cell density after 2 days of culture increased by 50% on gamma-treated surfaces, which reflected the 25% higher rate of cell proliferation. Osteoblasts on gamma-treated surfaces showed 30% higher alkaline phosphatase activity at day 5 and 60% higher calcium deposition at day 20 than non treated surface, while the strength of *in vivo* bone–implant integration on rats femur increased by 40% at the early healing stage of week 2 for gamma-treated implants. Gamma ray–treated surfaces regained hydrophilicity and showed a lower percentage of carbon (35%) as opposed to

48% on untreated aged surfaces. The data indicated that gamma ray pretreatment of titanium substantially enhances its bioactivity and osteoconductivity, in association with the significant reduction in surface carbon and the recovery of hydrophilicity. In conclusion, their results suggested that gamma ray treatment could be an effective surface enhancement technology to overcome biological aging of titanium and improve the biological properties of titanium implants.

Surface hydrophilicity preservation

Moreover, other authors have found that the combination of storage in physiological saline solution and gamma-ray irradiation can prevent the phenomenon of biological aging of titanium, avoiding the titanium surfaces to be contaminated over the time by hydrocarbons naturally present in the environment and consequently preserving hydrophilicity [26, 27]. Their studies showed that this process to protect titanium surface from the surrounding environment during production diminishes hydrocarbon contamination and enhances surface energy. Osteoblast-like cells cultured on these chemically purer and hydrophilic surfaces produced more differentiation markers highlighted by the increasement in cell layer of alkaline phosphatase specific activity and by osteocalcin relative expression.

1.2 Biological effectiveness of hyperhydrophilic surfaces

In the recent years, the biological and molecular mechanism through which surfaces with high hydrophilicity could drive to a better osseointegration have been studied and descripted in literature. A review on the known biological and clinical effects of hydrophilic implant surfaces has been proposed by Gittens et al. [28], from which we can assume that surface wettability affects different aspects of the implant-bone biological system, including:

- surface conditioning by protein and other macromolecules adsorbed on the surface;
- cellular interactions with the conditioned surface;
- timing and quality of osseointegration;
- bacterial adhesion and bio-film formation.

1.2.1 Surface conditioning

Surfaces influence protein adsorption in term of amount of adsorbed proteins, strength of bonding and tridimensional conformation. With particular regard to thes last aspect, we know from the literature that protein on hydrophobic surfaces tend to change their tridimensional structure in order to display their hydrophobic components so to be able to have a direct contact with the surface. This morphological modification is called 'partial unfolding' and it brings protein to lose also part of their function, together with their original form. The partial unfolding do not allow proteins to create a full functional bonding with surfaces, resulting in a less effective adsorption. Moreover,

the tridimensional modification of the protein structure could mask cellular adhesion receptor, which are necessary to create a functional interaction with the conditioned surface [28, 29, 30]. For example it has been demonstrated that fibronectin, a human blood protein which becomes part of the conditioning layer of implant surfaces and which have a major role in cell-adhesion when is adsorbed on a hydrophobic surface, is partially unfold and consequently lose part of its function, resulting in a less-effective surface-cell bridge [30, 31]. Concerning the strenght and the bonding of protein adsorbed, few datas are reported in literature and this aspect has been deeply investigated in this work.

1.2.2 Cells - surface interaction

Surfaces hydrophilicity plays a leading role also in implant-autologous cells interaction. As discussed in the previous paragraph, cells need a functional relationship between blood proteins and implant to obtain an effective adhesion on the surfaces as schematically shown in figure 1.4 [32]. In addition to this, the moderate immune response [33] and the lower activation of thrombocytes [34] found on hydrophilic surfaces compared to hydrophobic ones can facilitate the invasion and the mobilization of the blood clot by mesenchymal stem cells (MSCs) [35]. Numerous studies which aimed to evaluate the role of surface wettability on cells morphology, adhesion and proliferation, found that hydrophilic Ti/TiO2 promoted flattened morphologies and higher proliferation rates [23, 26, 36].

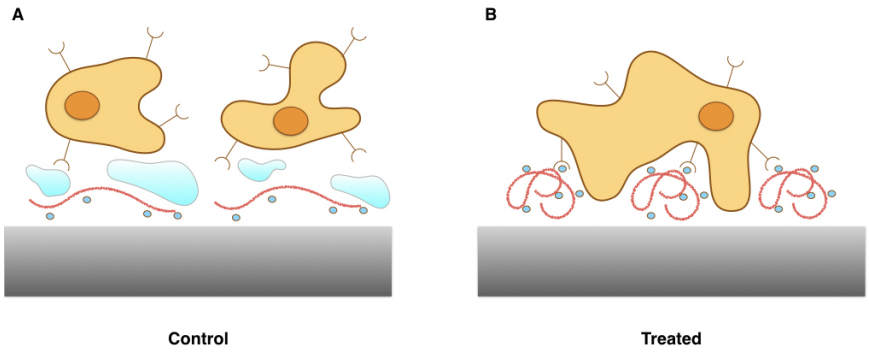

FIGURE 1.4: Diagram representing the rationale for obtaining hydrophilic titanium surfaces. Hydrophobic titanium surfaces cause the misfolding of proteins after their adsorption, and often induce the masking of cell-binding domains with consequently scarce adhesion of the circulating cells to the surface (A). Hydrophilic titanium surfaces avoid proteins misfolding during their adsorption and lead to a better cell adhesion and behavior (B).

1.2.3 Osseointegration

As discussed above, hydrophilicity plays a pivotal role in the contest of osseointegration, which is directly guided by the biological response of the surrounding milieu.

Preclinical model

The virtuous effects of surface wettability have been often demonstrated on animal models. Hydrophilic, relatively smooth experimental surfaces of Titanium implants promoted early bone formation compared to hydrophobic surfaces [12]. In a rat tibia model, the tissue covering the explanted devices revealed more cells positive for alkaline phosphatase (ALP) and for bone morphogenetic protein 2 (BMP-2) after 8 days on the hydrophilic surfaces compared to the hydrophobic ones. Moreover, comparable levels of ALP and osteocalcin (OCN), which are two early differentiation markes for osteoblasts, were found on both surfaces after 14 and 21 days of culture.

These findings suggest that hydrophilicity plays a major role in early stages of osseointegration, promoting osteoblastic differentiation.

In another work, Schwarz et al. evaluated the performance of hydrophilic roughened implants compared to roughened non-hydrophilic implants in the lower and upper jaw of dogs for 4 weeks [37]. The results confirmed the superior performance of superhydrophilic surfaces over hydrophobic surfaces, with higher bone-to-implant contacts after 1 week and up to 2 weeks before reaching similar levels, in the case of the lower jaw, or until the end of the study, in the case of the upper jaw. Elias et al. compared different experimental surfaces modified by blasting, acid etching or anodization in a 12 week rabbit tibial model [38]. Among the different groups, the anodized surfaces presented the highest hydrophilicity and despite having the lowest surface roughness they promoted the highest removal torque *in vivo*, suggesting that the effect of hydrophilicity could elicit a stronger response than surface roughness by itself *in vivo*. Taking advantage of the effects of photocatalysis on an anatase titanium dioxide coating, Hirakawa et al. obtained similar results [39]. They compared coated UV- treated (and thus hydrophilic) experimental Ti surfaces with uncoated, untreated ones by positioning them in a dog mandibular model. The photocatalytic treatment of the coating enhanced early osseointegration, being bone-to-implant contact significantly higher (42.7%) on test surfaces compared to controls (28.4%) after 2 weeks.

Clinical model

In the light of the results for animal models, Lang et al. pioneered the field in clinic and evaluated the rate and the degree of osseointegration of chemically modified moderately rough hydrophilic and hydrophobic implant surfaces during early phases of healing in humans [40]. The devices used for this study were either hydrophobic (SLA) or hydrophilic (SLActive) surface obtained through storage in physiological saline solution and gamma ray irradiation. The devices were surgically installed into the retro-molar area of 49 human volunteers and retrieved after 7, 14, 28 and 42 days of submerged healing. Histologic ground sections were prepared and histomorphometric analysis were performed to evaluate tissue components (i.e. old bone, new bone, bone debris and soft tissue) in contact with the device surfaces. All the device sites healed uneventfully and all the device surfaces were partially coated with bone debris. A significant fraction of this bone matrix coating became increasingly covered with newly formed bone. The process of new bone formation started already during the first week in the trabecular regions and increased gradually up to 42 days. The percentage of direct contact between newly formed bone and the device (bone-to-implant contact) after 2 and 4 weeks was more pronounced adjacent to the SLActive than to the SLA surface (14.8% vs. 12.2% and 48.3% vs. 32.4%, respectively), but after 42 days, these differences were no longer evident (61.6% vs. 61.5%). The healing showed similar characteristics with bone resorptive and appositional events for both SLActive and SLA surfaces between 7 and 42 days; however, the degree of osseointegration after 2 and 4 weeks was superior for the SLActive surface compared with the SLA surface, showing how higher wettabilities can provide faster osseointegration.

1.2.4 Bacterial adhesion

Finally, bacterial adhesion to implant surface represents one of the major issue in implantology, which severely influences osseointegration. Indeed microrganisms accumulation on titanium, which find an optimal micro-environment, often lead to peri-implantitis and to tardive implant failure.

Even though the mechanisms by which bacteria adhere to surfaces are not fully understood, several physicochemical surface properties of the material as well as of the bacteria themselves have been described to contribute to the initial adhesion process [41]. On the materials side, surface roughness as well as hydrophilicity and surface free energy are known to influence bacterial adhesion [42, 43].

According to Liu et al., bacterial adhesion may decrease or increase with increasing surface energy of substrates, depending on the physicochemical properties of the substrate, the bacterial strains tested and the solution used [44]. Consequently, surface hydrophilicity plays an important and elaborated role in biomaterial/bacterial interaction; however, systems are complex and influenced by a pattern of different factors which can interact with bacteria adeshion. In theory, hydrophobic bacterial strains will more likely adhere to biomaterials with hydrophobic surface properties, and correspondingly hydrophilic species will preferentially adhere to hydrophilic surfaces. Hydrophobic interactions are common and are involved in the mechanism of action of different microbial adhesion elements, such as hydrophobic cell membrane components as well as adhesins located on fimbria or pili [45]. Several studies have confirmed that

adhesion of the human pathogens *Staphylococcus aureus* and *S. epidermidis* is correlated to increased hydrophobicity of the biomaterial surface, and, more generally, that hydrophobicity is a major feature for bacterial adhesion [46].

In the clinical setting, however, the situation may be quite different. Quirynen et al. [47] compared oral biofilm development on hydrophobic (surface free energy of 20 erg/cm^2) and more hydrophilic (58 erg/cm^2) specimens in a clinical study over periods of up to 6 days. In this study, the hydrophobic material had significantly less plaque after 6 days. One of the main reasons for the poor correlation between theoretical thermodynamics of *in vitro* basic models and the more complex clinical situation is the formation of conditioning films *in vivo* that alter the surface properties of biomaterials as soon as they encounter biofluids. Bruinsma et al. [48] reported that the initial difference in wettability between hydrophilic and hydrophobic contact lenses, with water CAs of 57^o and 106^o, respectively, was reduced to 57^o and 69^o after contact with human tear liquid. The adsorbed tear films showed a different protein composition, as analyzed by sodium dodecyl sulfate–polyacrylamide gel electrophoresis (SDS-PAGE), which influenced subsequent bacterial adhesion. In another study, MacKintosh et al. [49] investigated the adhesion of S. epidermidis to polyethylene terephthalate samples with hydrophilic, hydrophobic and ionic charge surface modifications. When the adhesion experiments were performed in phosphate buffered saline, where the original surface state was maintained, nonspecific bacterial adhesion after 24 h was lower by more than one order of magnitude on the hydrophilic modification in comparison to the unmodified control and the other modified surfaces.

After incubation in serum, however, the control, hydrophilic and hydrophobic surfaces showed comparable, very low bacterial adhesion, while the cationic and anionic modifications instead showed substantially higher amounts of bacterial adhesion. As stated by the authors, serum proteins are more likely to exert a greater effect on the surface adhesion and biofilm formation of *S. epidermidis* in vivo than nonspecific interactions. Since *S. epidermidis* and many other bacteria have developed specific adhesion mechanisms to certain blood proteins, like fibrinogen or fibronectin [49], biomaterial surface properties that lead to conformational changes of these proteins during surface adsorption [50] will probably also influence bacterial adhesion. Hence, even if surface free energy and surface charge are in fact the determinants of bacterial adhesion, the indirect influences of these parameters, coupled to changes in the chemical composition, the molecule conformation in the conditioning film and the presence of nanoscale features on the surface, are still not fully understood or predictable. As a result, anti-adhesive strategies based on physicochemical and thermodynamic approaches have only been partly successful so far, though they are still among the most attractive tools used to combat the costly and burdensome bacterial complications.

1.3 Titanium biological aging

Biocompatibility, which is a critical factor in bone-implant integration, depends on surface physicochemical properties such as surface topography, wettability, and chemical composition [26]. One of the current problems of dental implant therapy is incomplete integration, being the reported bone to implant contact (BIC) percentage $45\% \pm 16\%$ [51] or 50-65% [52].

As previously discussed, many studies have correlated improved osseointegration with wettability modification characteristics other than hydrophilicity. These studies demonstrated the correlation between osseointegration and the amount of hydrocarbon adsorbed on the surface, showing in fact that the osteoconductive capacity of titanium implants increased after 4 weeks in a rat femoral model as a function of hydrocarbon removal after UV treatment rather than with the level of hydrophilicity, and indicated that the amount of hydrocarbon adsorbed on the surface at the time of implantation was crucial in determining the bone-to-implant integration [23]. This implies a critical role for surface contamination of titanium implants not only for the wetting behavior but also for the biological outcome. Surface wettability is strongly affected by hydrocarbon deposition but even when super hydrophilicity is acquired, it does not guarantee a surface free from any contamination [53]. Hayashi et al. studied the effect of hydrocarbon deposition on osteoblastic cells activity and observed how this surface contamination can affect implant osseointegration [20]. Calcium deposition, which is representative of osteoconductivity, decreased by 40% on surfaces with a C/Ti rate

of 1. as well as the expression of ALP decreased by 50%. Therefore, the bone-titanium integration of a carbon-coated surface may be reduced by half compared with that of an uncontaminated surface. The presence of hydrocarbons on the surface influences *in vitro* osteoconductivity, and resulted from a decrease in protein adsorption, a decrease in osteoblastic cell attachment, and suppression of cell spreading, which are closely interrelated processes.

Other stuedies demonstrated that titanium constantly absorbs organic molecules, such as polycarbonyls and hydrocarbons, from the atmosphere, water, and cleaning solutions [14, 54], and as a consequence the frequent detection of high levels of carbon on titanium surfaces indicates that such contamination may be unavoidable [10, 27]. Reports have suggested a link between surface hydrocarbons deposition and the hydrophilicity of titanium. Indeed, the contact angle of H2O has been found to increase with increased absorption of hydrocarbons [55]. Aita et al. [23] measured the hydrocarbon deposition-related loss of wettability of two different implant surfaces occuring over the time and found out that hyperhydrophilic surfaces completely lose their wettability after 30 days of storage. Detailed analyses of the surface energy, electric charge, and other physicochemical properties are also required to identify the mechanism underlying osseointegration; however, the results of this study suggest that removal of hydrocarbons may be an important step in promoting the bioactivity and osseointegration of titanium. As previously reported ultraviolet treatment [56], gamma-ray irradiation [25] and storage in physiological saline solution [26, 27] could promote osteoblastic differentiation and growth factor production, thereby enhancing bone-implant integration while maintaining low carbon

contamination of the implant surface. At the light of what we said, it becomes fundamental to find strategies not only to obtain superhydrophilic titanium surfaces, but also to preserve contamination with hydrocarbons and consequently titanium biological aging.

Bibliography

[1] Branemark PI, Hansson BO, Adell R, Breine U, Lindstrom J, Hallen O, et al. *Osseointegrated implants in the treatment of the edentulous jaw. Experience from a 10-year period.* Scand J Plast Reconstr Surg Suppl 1977;16:1–132.

[2] Branemark PI, Adell R, Breine U, Hansson BO, Lindstrom J, Ohlsson A. *Intra- osseous anchorage of dental prostheses. I. Experimental studies.* Scand J Plast Reconstr Surg. 1969;3(2):81–100.

[3] Adell R, Lekholm U, Rockler B, Branemark PI. *A 15-year study of osseointegrated implants in the treatment of the edentulous jaw.* Int J Oral Surg. 1981;10(6):387–416.

[4] Meyer U, Joos U, Mythili J, Stamm T, Hohoff A, Fillies T, et al. *Ultrastructural characterization of the implant/bone interface of immediately loaded dental implants.* Biomaterials. 2004;25(10):1959–67.

[5] Szmukler-Moncler S, Piattelli A, Favero G, Dubruille JH. *Considerations preliminary to the application of early and immediate loading protocols in dental implantology.* Clin Oral Implants Res. 2000;11(1):12–25.

[6] Davies J. *Understanding peri-implant endosseous healing.* J Dent Educ. 2003;67(8): 932–49.

[7] Raghavendra S, Wood MC, Taylor TD, Raghavendra S Taylor TD, WMC, Raghavendra S, Wood MC, et al. *Early wound healing around endosseous implants: a review of the literature.* Int J Oral Maxillofac Implants. 2005;20(3):425–31.

[8] Albrektsson T, Zarb G, Worthington P, Eriksson AR. *The long-term efficacy of currently used dental implants: a review and proposed criteria of success.* Int J Oral Maxillofac Implants. 1986;1(1):11–25.

[9] Wennerberg A., Albrektsson T., *Effects of titanium surface topography on bone integration: a systematic review.* Clin Oral Implants Res 2009;20:172-184.

[10] Massaro C, Rotolo P, De Riccardis F, Milella E, Napoli A, Wieland M *Comparative investigation of the surface properties of commercial titanium dental implants. Part I. Chemical composition.* J Mater Sci Mater Med 2002;13:535–48.

[11] Le Guehennec L, Soueidan A, Layrolle P, Amouriq Y. *Surface treatments of titanium dental implants for rapid osseointegration.* Dent Mater 2007;23:844–54.

[12] Eriksson C, Nygren H, Ohlson K. *Implantation of hydrophilic and hydrophobic titanium discs in rat tibia: cellular reactions on the surfaces during the first 3 weeks in bone.* Biomaterials 2004;25:4759–66.

[13] Bornstein MM, Valderrama P, Jones AA, Wilson TG, Seibl R, Cochran DL. *Bone apposition around two different sandblasted and acid-etched titanium implant surfaces: a histomorphometric study in canine mandibles.* Clin Oral Implants Res 2008;19:233–41.

[14] Kilpadi DV, Lemons JE. *Surface energy characterization of unalloyed titanium implants.* J Biomed Mater Res 1994;28:1419–25.

[15] Kohavi D, Badihi HL, Rosen G, Steinberg D, Sela MN. *Wettability versus electrostatic forces in fibronectin and albumin adsorption to titanium surfaces.* Clin Oral Implants Res 2013;24:1002–8.

[16] Rupp F, Scheideler L, Rehbein D, Axmann D, Gels-Gerstorfer J. *Roughness induced dynamic changes of wettability of acid etched titanium implant modifications.* Biomaterials 2004;25:1429–38.

[17] Rupp F, Scheideler L, Eichler M, Geis-Gerstorfer J. *Wetting behavior of dental implants.* Int J Oral Maxillofac Implants 2011;26:1256–66.

[18] Boyan BD, Hummert TW, Dean DD, Schwartz Z. *Role of material surfaces in regulating bone and cartilage cell response.*Biomaterials. 1996;17(2):137–146.

[19] Guo CY, Matinlinna JP, Hong Tang AT. *Effects of surface charges on dental implants: past, present, and future.* International Journal of Biomaterials, vol. 2012, Article ID 381535, 5 pages, 2012.

[20] Hayashi R Ueno T, Migita S, Tsutsumi Y, Doi H, Ogawa T, Hanawa T, Wakabayashi N. *Hydrocarbon deposition attenuates osteoblast activity on titanium* J Dent Res 2014;93(7):698-703

[21] Lee JH, Ogawa T. *The biological aging of titanium implants.* Implant Dent. 2012;21(5):415-21.

[22] Kaneko M., Okura I., *Photocatalysis: science and technology.* Springer 2002.

[23] Aita H, Hori N, Takeuchi M, Suzuki T, Yamada M, Anpo M, Ogawa T. *The effect of ultraviolet functionalization of titanium on integration with bone.* Biomaterials. 2009;30(6):1015–1025.

[24] Hori N, Ueno T, Suzuki T, Yamada M, Att W. *Ultraviolet light treatment for the restoration of aged-related degradation of titanium bioactivity.* Int J Oral Maxillofac Implants 2010;25:49–62.

[25] Ueno T, Takeuchi M, Hori N, Iwasa F, Minamikawa H, Igarashi Y, et al. *Gamma ray treatment enhances bioactivity and osseointegration capability of titanium.* J Biomed Mater Res B Appl Biomater 2012 100:2279-2287.

[26] Zhao G, Schwartz Z, Wieland M, Rupp F, Geis-Gerstorfer J, Cochran DL *High surface energy enhances cell response to titanium substrate microstructure.* J Biomed Mater Res 2005;74A:49–58.

[27] Buser D, Broggini N, Wieland M, Schenk RK, Denzer AJ, Cochran DL, et al. *Enhanced bone apposition to a chemically modified SLA titanium surface.* J Dent Res 2004 83:529-533.

[28] Gittens RA, Scheideler L, Rupp F, Hyzy SL, Geis-Gerstorfer J, Schwartz Z, Boyan BD. *A review on the wettability of dental implant surfaces II: Biological and clinical aspects.* Acta Biomaterialia 10 (2014) 2907–2918.

[29] Vogler EA. *Protein adsorption in three dimensions.* Biomaterials 2012;33:1201–37.

[30] Wilson CJ, Clegg RE, Leavesley DI, Pearcy MJ. *Mediation of biomaterial–cell interactions by adsorbed proteins: a review.* Tissue Eng 2005;11:1–18.

[31] Salasznyk RM, Williams WA, Boskey A, Batorsky A, Plopper GE. *Adhesion to vitronectin and collagen I promotes osteogenic differentiation of human mesenchymal stem cells.* J Biomed Biotechnol 2004;2004:24–34.

[32] Huang QL, Lin LX, Yang Y, Hu R, Vogler EA, Lin CJ. *Role of trapped air in the formation of cell-and-protein micropatterns on superhydrophobic/ superhydrophilic microtemplated surfaces.* Biomaterials 2012;33:8213–20.

[33] Kou PM, Schwartz Z, Boyan BD, Babensee JE. *Dendritic cell responses to surface properties of clinical titanium surfaces.* Acta Biomater 2011;7:1354–63.

[34] Brogren H, Karlsson L, Andersson M, Wang L, Erlinge D, Jern S. *Platelets synthesize large amounts of active plasminogen activator inhibitor 1.* Blood 2004;104:3943–8.

[35] Davies JE. *In vitro modeling of the bone/implant interface*. Anat Rec 1996;245:426–45.

[36] Sawase T, Jimbo R, Baba K, Shibata Y, Ikeda T, Atsuta M. *Photo-induced hydrophilicity enhances initial cell behavior and early bone apposition.* Clin Oral Implants Res 2008;19:491–6.

[37] Schwarz F, Ferrari D, Herten M, Mihatovic I, Wieland M, Sager M. *Effects of surface hydrophilicity and microtopography on early stages of soft and hard tissue integration at non-submerged titanium implants: an immunohistochemical study in dogs.* J Periodontol 2007;78:2171–84.

[38] Elias CN, Oshida Y, Lima JH, Muller CA. *Relationship between surface properties (roughness, wettability and morphology) of titanium and dental implant removal torque.* J Mech Behav Biomed Mater 2008;1:234–42.

[39] Hirakawa Y, Jimbo R, Shibata Y, Watanabe I, Wennerberg A, Sawase T. *Accelerated bone formation on photo-induced hydrophilic*

titanium implants: an experimental study in the dog mandible. Clin Oral Implants Res 2013;24:139–44.

[40] Lang NP, Salvi GE, Huynh-Ba G, Ivanovski S, Donos N, Bosshardt DD. *Early osseointegration to hydrophilic and hydrophobic implant surfaces in humans.* Clin Oral Implants Res 2011;22:349–56.

[41] An YH, Friedman RJ. *Concise review of mechanisms of bacterial adhesion to biomaterial surfaces.* J Biomed Mater Res 1998;43:338–48.

[42] Drake DR, Paul J, Keller JC. *Primary bacterial colonization of implant surfaces.* Int J Oral Maxillofac Implants 1999;14:226–32.

[43] Quirynen M, Bollen CM. *The influence of surface roughness and surface-free energy on supra- and subgingival plaque formation in man. A review of the literature.* J Clin Periodontol 1995;22:1–14.

[44] Liu Y, Zhao Q. *Influence of surface energy of modified surfaces on bacterial adhesion.* Biophys Chem 2005;117:39–45.

[45] Doyle RJ. *Contribution of the hydrophobic effect to microbial infection.* Microb Infect 2000;2:391–400.

[46] Oliveira R, Azeredo J, Teixeira P, Fonseca AP. *The role of hydrophobicity in bacterial adhesion.* In: Gilbert P, Allison D, Brading M, Verran J, Walker J, editors. Biofilm community interactions: chance or necessity? Cardiff: Bioline; 2001. p. 11–22.

[47] Quirynen M, Marechal M, Busscher HJ, Weerkamp AH, Darius PL, van Steenberghe D. *The influence of surface free energy and surface roughness on early plaque formation. An in vivo study in man.* J Clin Periodontol 1990;17:138–44.

[48] Bruinsma GM, van der Mei HC, Busscher HJ. *Bacterial adhesion to surface hydrophilic and hydrophobic contact lenses.* Biomaterials 2001;22: 3217–24.

[49] MacKintosh EE, Patel JD, Marchant RE, Anderson JM. *Effects of biomaterial surface chemistry on the adhesion and biofilm formation of Staphylococcus epidermidis in vitro.* J Biomed Mater Res A 2006;78:836–42.

[50] Keselowsky BG, Collard DM, Garcia AJ. *Surface chemistry modulates fibronectin conformation and directs integrin binding and specificity to control cell adhesion.* J Biomed Mater Res A 2003;66A:247–59.

[51] Weinlaender M, Kenney EB, Lekovic V, Beumer J, Moy PK, Lewis S. *Histomorphometry of bone apposition around three types of endosseous dental implants.* Int J Oral Maxillofac Implants. 1992 Winter;7(4):491-6.

[52] Ogawa T, Nishimura I. *Different bone integration profiles of turned and acid-etched implants associated with modulated expression of extracellular matrix genes.* Int J Oral Maxillofac Implants. 2003 Mar-Apr;18(2):200-10.

[53] Hashimoto K, Irie H, Fujishima A. *TiO2 photocatalysis: a historical overview and future prospects.* Jpn J Appl Phys Part 1 2005;44:8269–85.

[54] Serro AP, Saramago B. *Influence of sterilization on the mineralization of titanium implants induced by incubation in various biological model fluids.* Biomaterials 2003 24:4749-4760.

[55] Takeuchi M, Sakamoto K, Martra G, Coluccia S, Anpo M. *Mechanism of photoinduced superhydrophilicity on the TiO2 photocatalyst surface.* J Phys Chem B 2005 109:15422-15428.

[56] Att W., Ogawa T. *Biological aging of implant surfaces and their restoration with ultraviolet light treatment: a novel understanding of osseointegration.* Int J Oral Maxillofac Implants. 2012 Jul-Aug;27(4):753-61.

Chapter 2

Aims

Surfaces characteristics of dental implants have a strong influence on the biological response occuring after implant placement, consequently affecting osseointegration. In the last years, this topic has been very popular in dental biomaterial research and many authors developed and studied different methods to ameliorate dental implant performances and their effects on bone cells proliferation, adhesion and morphology, together with protein adsorption.

Considering this, the aim of the thesis was the development of a method to obtain hydrophilic titanium surfaces, starting from two different commercially available titanium implant surfaces, and to characterize them from a chemical, physical, morphological, biochemical and cellular point of view. The method developed is not revealed in this work because is actually under patent application, therefore the experimental part of this work will focus only on the analysis of the surfaces and is composed by four chapters:

- in Chapter 3 we analyzed the biological response of MC3T3-E1 cells on two commercially available surfaces to characterize the surfaces used in the subsequent studies;

- in Chapter 4 we studied chemical-physical and morphological modifications occuring on the surfaces following our treatment method, togheter with the resulting capability of adsorbing proteins;

- in Chapter 5 we compared MC3T3-E1 cells response on treated and non-treated surfaces, in order to fully understand the effects of our treatment on bone cells behaviour;

- Chapter 6 includes the conclusions and future perspectives of this work.

Part II

Experiments

Chapter 3

Machined and ZirTi® surfaces characterization and murine MC3T3-E1 cells biological response

3.1 Introduction

The surface characteristics of dental titanium implants play a major role during the biologic response of the surrounding milieu that follows implant placement [1]. In particular, osseointegration depends on the first response of cells to the substrate, which in turn depends on the chemical, physical and morphological characteristics of the surfaces and by how these features influence protein adsorption at the interface [2].

In implant dentistry, two morphologically different titanium surfaces are commonly used: machined and sand blasted and acid-etched. Machined implants present a smooth surface and were the first class of implant used in dentistry. On the other hand, acid etched and sand

blasted implants are manifactured in order to present a rough surface texture. In the last two decades, rough surfaces had been more frequently used in clinical practice, because of their favorable characteristics. In fact, *in vitro* experiments demonstrated that osteoblast proliferation and adhesion were enhanced on rough surfaces, as well as osteoblasts differentiation [3, 4, 5]. Similarly, in vivo tests have demonstrated that rough textures allow a faster osseointegration [1].

Moreover, clinical studies and systematic reviews have indicated a positive correlation between surface roughness and bone-implant contact [6]. This led to progressively abandon smoother surfaces used in the early implant systems for rougher topographies and to focus on those specific roughening treatments that appeared to promote bone formation more effectively.

However, rough surfaces are not completely exempt from issues. First of all, the main problem connected to the use of these implant is the easier development of peri-implantitis, if compared to smooth implant surfaces, caused by the accumulation of pathogenic microorganisms on titanium microtexture and which can lead to late implant failure. In fact, a review by Esposito and colleagues showed that smooth surfaces have a 20% reduction in risk of being affected by perimplantitis over a 3 year-period, if compared to rough implant surfaces [7, 8]. Consequently in the last years, implant dentistry observed a rapprochement to smooth surfaces, that are seen as a possible tool to face the issue of perimplantitis. Concerning with this, the aim of this experimental chapter was to evaluate any difference in protein adsorption on a smooth or rough commercially available

titanium surface, and how different topographical patterns could affect the subsequent behavior of murine osteoblasts in terms of proliferation, viability and adhesion.

3.2 Materials and methods

3.2.1 Titanium discs

Commercially pure, grade 4 (ISO5832/2) titanium discs of 8.0mm of diameter and 3.5mm thickness, were kindly provided from Sweden&Marina (Due Carrare, PD, Italy) and used in this study. Half of the discs were machined and not treated at the end of the milling process, while the other half were acid-etched and sandblasted following the procedure used by Sweden&Martina to obtain ZirTi® implant surface. All titanium discs were cleaned in an Argon-activated plasma reactor and sterilized, following the procedure used for commercial implants.

3.2.2 Discs characterization

Discs properties were evaluated from a physical, chemical and morphological point of view. A 5µl bead of water was dropped on the surfaces and standardized photographs were taken. Subsequently the contact angle between titanium surfaces and the water drop was measured through the ImageJ software (ImageJ, U. S. National Institutes of Health, Bethesda, MD, USA). An X-ray Photoelectron Spectroscopy analysis (XPS) was performed at 20eV in order to detect chemical species on the surfaces, while a scanning electron microscopy analysis (SEM) was used to observe titanium surface morphology.

Discs were observed using a dual beam Zeiss Auriga Compact system equipped with a GEMINI Field-Effect SEM column (Zeiss, Oberkochen, Germany), by performing the analysis at 5 keV.

3.2.3 Protein adsorption

To study the influence of titanium surfaces on protein adsorption, a qualitative and quantitative analysis was performed. Titanium discs were soaked for 2 hours in a 200g/ml Fetal Bovine Serum (FBS, Life Technologies, Carlsbad, CA; USA) solution. The amount of protein adsorbed was subsequently quantitated through the Bradford assay (BIO-RAD Protein Assay, BIO-RAD, Hercules, CA, USA) following manufacturer's recommendation. Briefly, 10µl of supernatants were mixed with 200µl of Bradford solution, and after a 2 minutes of incubation at 37°C, sample absorbance was measured at 620nm with the plate-reader (Multiskan FC, Thermo Fisher Scientific, Waltham, MA, USA). Subsequently, titanium discs were rinsed two times in PBS (Phosphate Buffer Saline, Life Technologies) and treated with 80µl of Sample Buffer (Tris-HCl 62.5mM pH 6.8, SDS 1.5% w/v, DTT 100mM and traces of Bromophenol Blue) to desorb proteins. Proteins were then freezed overnight, sonicated for 15 minutes, boiled at 95°C for 10 minutes and finally electrophorased on a 12% poly-acrylamide gel (Acrylamide/Bis-Acrylamide 30%, Sigma-Aldrich, Saint-Louis, MI; USA) at 180V constant for 1 hour. Proteins on gel were finally revealed through the Silver Stain (Sigma-Aldrich).

3.2.4 Cell culture

Murine osteoblasts MC3T3-E1 were obtained from the American Type Culture Collection and used for the in vitro assays. Cells were cultured in complete Alpha-MEM (Alpha MEM, Life Technologies) with the addiction of 10% FBS and of 1% Penicillin and Streptomycin (Pen-Strep, Life Technologies). *In vitro* assays were all performed in 48-well plates (JET BIOFIL, Guangzhou, China): titanium discs were positioned on the well bottom and cells were seeded above at a density of 10000cells/disc.

3.2.5 Cell viability

Cell viability was assayed through the use of Calcein AM. Forty-eight hours after seeding, culturing medium was removed and substituted with 500µl of a 4µM Calcein AM (Calcein AM, Sigma Aldrich) and 5µg/ml DAPI (DAPI, Life Technologies) solution in PBS. Samples were incubated at room temperature (RT) in dark conditions for 10 minutes and subsequently fixed with a 4% paraformaldheyde solution (PFA, Sigma-Aldrich) for 20 minutes in dark conditions at RT. Discs were observed with a stereomicroscope equipped for fluorescence (SMZ25, Nikon, Tokyo, Japan) and three range of interest areas (ROI) were chosen to quantify the amount of viable cells on each area with the ImageJ.

3.2.6 Cell metabolic activity

To observe cell metabolic activity and proliferation on different titanium surfaces, a Resazurin Sodium Salt assay was performed at different experimental points. Twenty-four, 48 and 72 hours after seeding culturing medium was removed and substituted with 500µl

of a serum-free medium; 100µl of the Resazurin Sodium Salt stock solution (final concentration 0.15mg/ml) were then added and samples incubated at 37°C and 5% CO_2 for 4 hours. Fluorescence was exited at 560nm and emitted at 585nm with a Multiskan Ascent microcell plate reader (Thermo Labsystems, Helsinki, Finland).

3.2.7 Cell morphology

Cell morphology was investigated through cytofluorescence and SEM. For fluorescence, after 24 hours cells were fixed in 4% PFA for 10 minutes at RT, rinsed twice in PBS and permeabilized with a 0.1% v/v Triton X-100 (Sigma-Aldrich) solution for 5 minutes at RT. To block non specific sites, after two rinses in PBS, samples were incubated in a 1% Bovine Serum Albumine (BSA, Sigma-Aldrich) solution for 30 minutes at RT. An anti-Vinculin monoclonal antibody, clone 7F9 (FAK100, Merck Millipore, Darmstadt, Germany) was applied 1:100 diluted in 1% BSA for 1 hour at RT to stain focal adhesion and subsequently revealed with a secondary anti-rabbit antibody labeled with the AlexFluor®488 (Life Technologies) 1:200 diluted. Simultaneously, TRITC-conjugated phalloidin (FAK100, Merck Millipore) 1:200 diluted was used to reveal actin filaments. Finally, after three washes with PBS, cell nuclei were revealed by incubation with DAPI (FAK100, Merck Millipore) for 5 minutes at RT. Images were taken with a stereomicroscope equipped for fluorescence (SMZ25, Nikon). SEM preparation was performed at RT 24 hours after seeding. Cells were rinsed in PBS, fixed with a 2.5% gluteraldehyde solution (Sigma-Aldrich) in Na-Cacodylate buffer (Sigma-Aldrich) for 30 minutes, washed in Na-Cacodylate for 5 minutes and dehydrated in ethanol at increasing concentration (Sigma-Aldrich). Samples were

finally critical point dried with the liquid carbon dioxide (CPD 030 Baltic, Walrus, Germany) and sputtered with a thin layer of gold through a SCD 040 coating device (Balzer Union). Microphotographs were taken using a dual beam Zeiss Auriga Compact system equipped with a Gemini Field-Effect SEM column (Zeiss). SEM analysis was performed at 5 keV.

3.2.8 Real time PCR

Total RNA was extracted from cell cultures using TriZol (Life Technologies, Carlsbad, CA, USA), according to the manufacturer's indications. TaqMan quantitative RT-PCR was performed using the following primer probe sets from Life Technologies (Carlsbad, CA, USA): Alkaline Phosphatase (ALP, Mm00475834 m1); Osteoprotegerin (OPG, Mm00435454 m1); Osteopontin (OPN Mm00436767 m1); Osteocalcin (for 5' - GCTGCGCTCTGTCTCTCTGA - 3'; rev 5' - TGC TTGGACATGAAGGCTTTG - 3' ;probe 5' - FAM-AAGCCCAGCGGCC - NFQ-3'); Cyclin D1 (CKD1, Mm00432359 m1); Vinculin (VCL, Mm004 47745 m1); the housekeeping gene used in the study was mouse GAPDH (Mm99999915 g1). qPCR was performed with a StepOne Real Time PCR machine (Life Technologies, Foster City, CA, USA).

3.2.9 Statistical analysis

Data were analyzed using Prism 6 (GraphPad, La Jolla, CA; USA). All the values are reported as the mean $\pm$ SD of three repeated experiments. Differences between groups were evaluated with the two-way ANOVA statistical test and Bonferroni's multiple comparison as post-test analysis. Differences were considered significant when $p<0.05$.

3.3 Results

3.3.1 Surface characteristics

A SEM analysis was performed to evaluate the micro topographic profile of the discs. Acid-etching and sandblasting treatment created a micro roughness texture on the discs (fig.3.1 A-B) and which significatively decreased surface wettability (fig.3.3 A-B, 3.4). Although the treatments affected the morphological and physical characteristics of the discs, they did not significantly alter their surface chemical composition as assessed by XPS (fig.3.2).

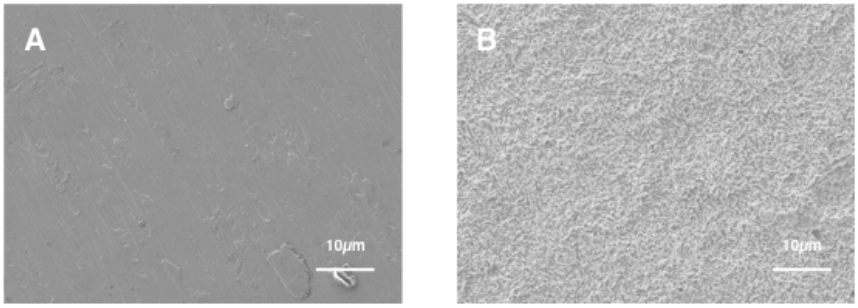

FIGURE 3.1: Typical SEM images of machined and ZirTi® surfaces microtopography.

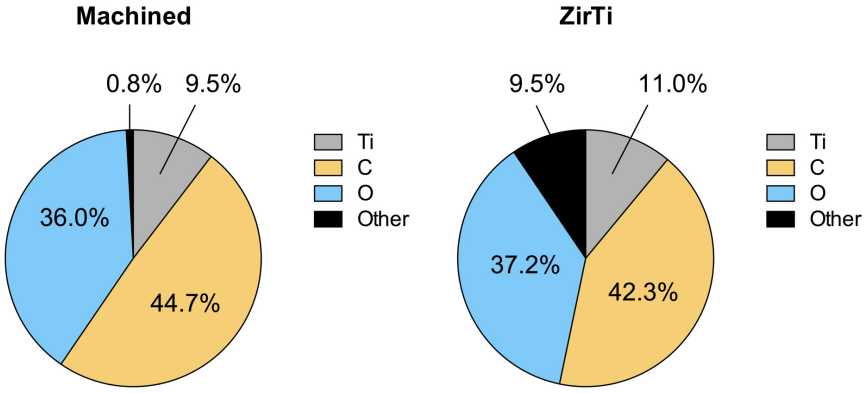

FIGURE 3.2: Chemical composition of machined and ZirTi® surfaces analyzed through XPS.

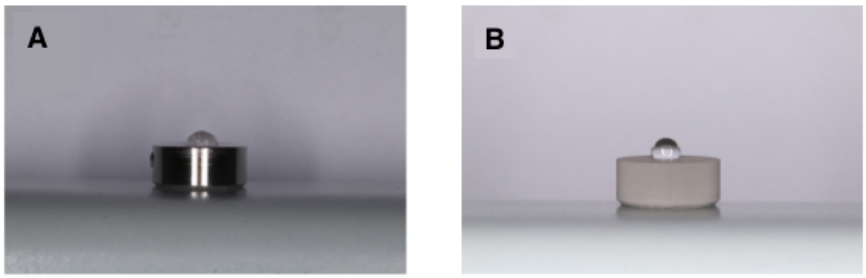

FIGURE 3.3: Standardized photograph of machined and ZirTi® surfaces wettability measurement.

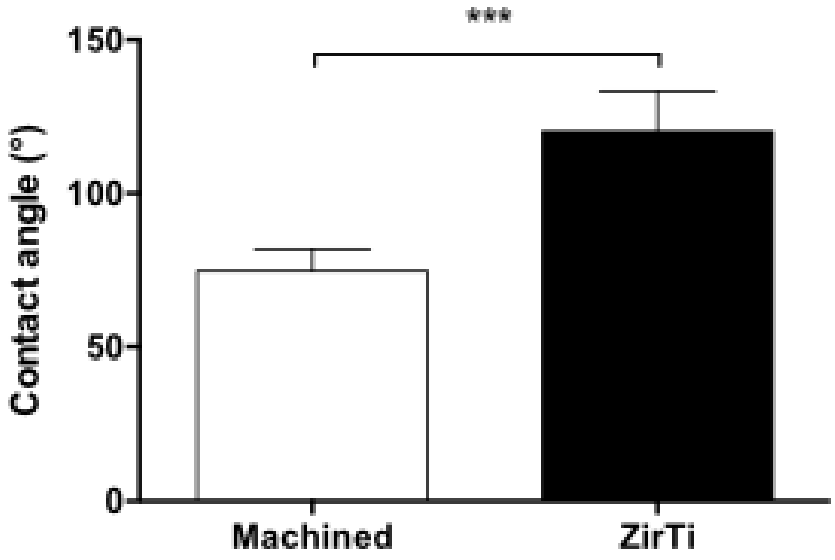

FIGURE 3.4: Histogram showing contact angle measurement on machined and ZirTi® surfaces. ***=p<0.001.

3.3.2 Protein adsorption

To investigate whether proteins were better adsorbed on a surface than on another, the amount of adsorbed proteins was quantitated through the Bradford assay. Both surfaces adsorb a similar amount of proteins with no statistically significative differences. A mean of 9.72 ± 0.82 µg and of 10.85 ± 2.01 µg of serum proteins were respectively adsorbed on machined and ZirTi® disc (fig.3.5). After the rinse in PBS, the SDS-PAGE analysis (fig.3.6) revealed that little more proteins remain attached on machined surface than on the ZirTi®, however different patterns were detected on the surfaces. Interestingly, a 150 kDa band was clearly marked on machined discs, while it was barely visible on ZiTi samples and similarly an approximately 60kDa band was more strongly marked on machined surfaces Furthermore, bands clearly detectable on ZirTi® surfaces were not revealed on machined discs (black arrows fig.3.6).

FIGURE 3.5: Amount of protein adsorbed on machined and ZirTi® surfaces.

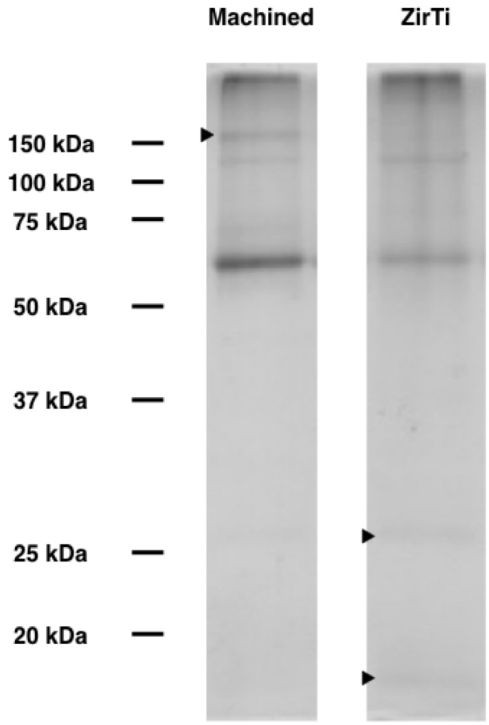

FIGURE 3.6: SDS-PAGE of protein adsorbed on machined and ZirTi® surfaces. Black arrows indicate proteins revealed only on one type of surface.

3.3.3 Cell proliferation

To observe how cells colonize the two different surfaces, Calcein AM staining was used. The entire titanium surface was analyzed and three representative and ROIs were chosen to determine the percent of surface covered by cells. Figure 3.8 shows that cells proliferated significantly faster on machined surfaces than on ZirTi®. This was confirmed through the analysis of cell metabolic activity after 24, 48 and 72 hours of culture through the Resazurin Sodium salt assay. After 48 hours the differences between the groups were already significative (Fig. 3.7).

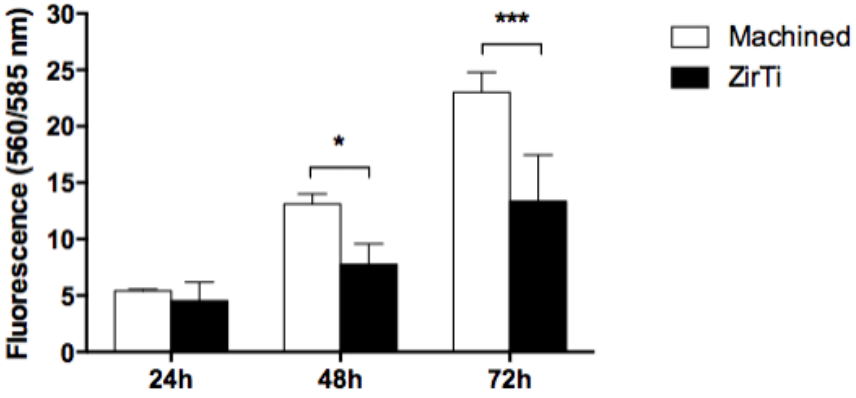

FIGURE 3.7: Histograms showing cell proliferation on machined and ZirTi® surfaces measured through Resazurine Sodium Salt assay for 24, 48 and 72h after seeding. *=p<0.05; ***=p<0.002.

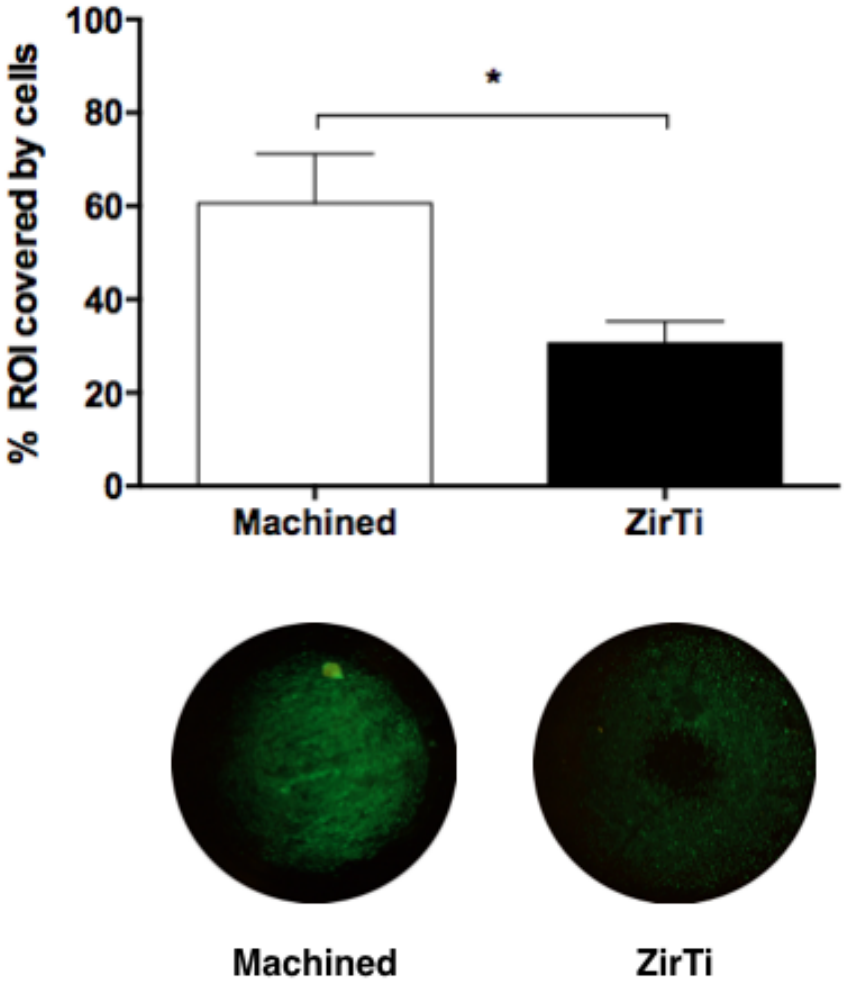

FIGURE 3.8: Histogram and relative images showing cell proliferationon machined and ZirTi® surfaces. *=p<0.05.

3.3.4 Cell distribution and organization during the adhesion

The morphology, adhesion and distribution of cells on titanium discs were analyzed through cytofluorescence and through the SEM. Figure 3.9 shows that cells on machined discs mostly aligned along the grooves of the surface (fig.3.9A and fig.3.9C), while cells on the ZirTi® were randomly distributed across the whole sample (fig.3.9 B and fig.3.9D). Both cytofluorescence (fig.3.9A-B) and SEM analysis (fig.3.9C-D) revealed that cells were healthy and with a quadrangular shape typical of osteoblast. SEM analysis (fig.3.9C-D) showed flatter cells both on the machined and on the ZirTi®. Taken together, these data demonstrate a strictly adhesion of murine osteoblasts to both surfaces.

3.3.5 Cell differentiation

We then proceeded to assess osteoblastic differentiation on Machined or ZiTi surfaces after 7 and 14 days of culture (fig.3.10 and fig.3.11). After 7 days of culture cells on ZiTi surfaces expressed higher levels of transcript for OPG and OCN (fig.3.10), tended to express lower levels of mRNA for Cyclin D1 and comparable levels of ALP and OPN. By 14 days however, higher levels of ALP, OPG, OPN and OCN in cells on ZirTi® surfaces were observed, together with comparable levels of Cyclin D1 and Vinculin (fig.3.11).

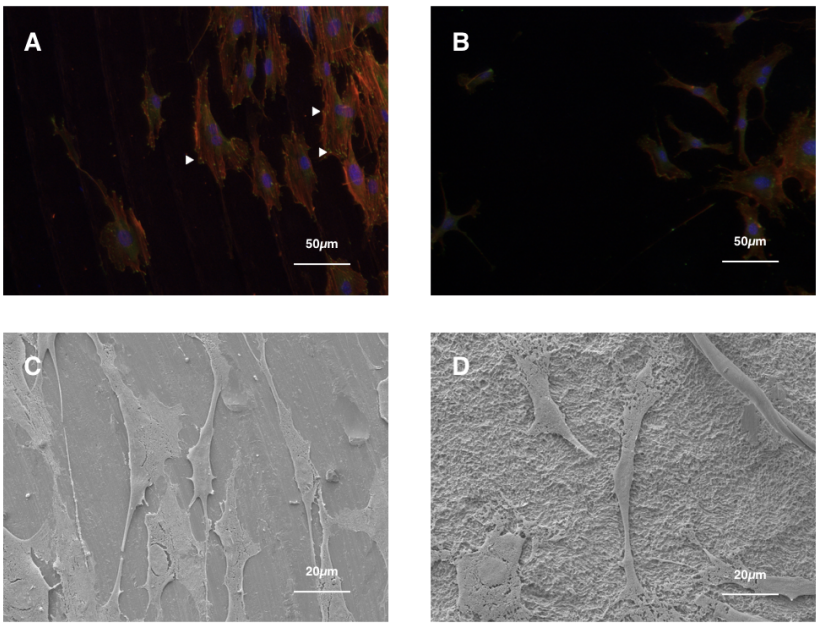

FIGURE 3.9: Typical fluorescence images showing MC3T3-E1 cells on machined (A) and ZirTi®(B) surfaces, staining for cytoskeleton (red), focal adhesion (green) and cell nuclei (blue). White arrows indicate evident focal adhesion. Typical SEM images showing MC3T3-E1 cells on machined (C) and ZirTi®(D) surfaces.

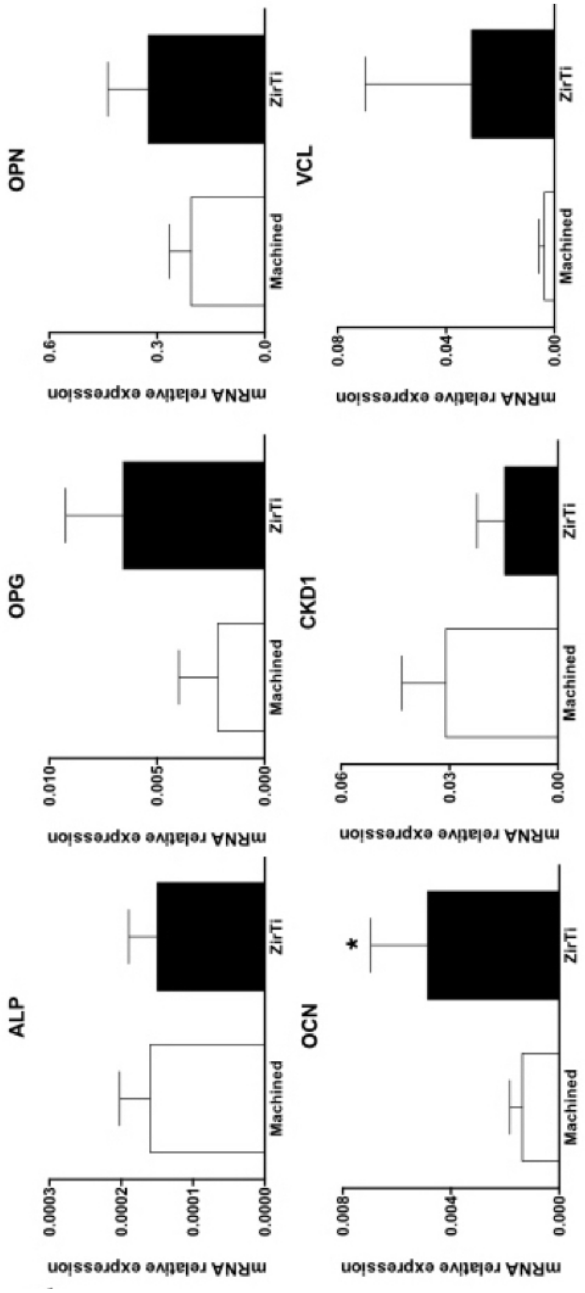

FIGURE 3.10: Real Time-PCR analysis: mRNA relative expression of alkaline phosphatase (ALP), osteoprotegerin (OPG), osteopontin (OPN), osteocalcin (OCN), ciclyin dependent kinase 1 (CKD1) and vinculin (VCL) after 7 days of culture.

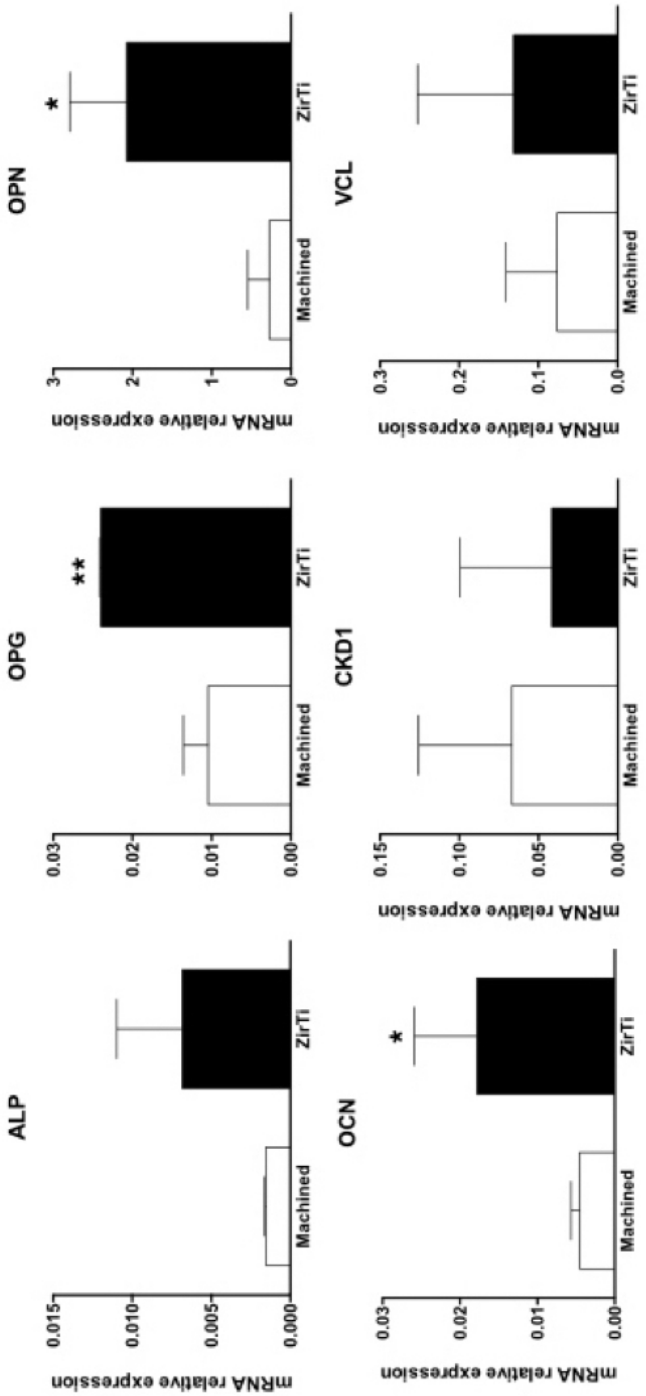

FIGURE 3.11: Real Time-PCR analysis: mRNA relative expression of alkaline phosphatase (ALP), osteoprotegerin (OPG), osteopontin (OPN), osteocalcin (OCN), ciclyin dependent kinase 1 (CKD1) and vinculin (VCL) after 14 days of culture.

3.4 Discussion

Rough titanium surfaces have been long considered the best option to improve implant integration due to the massive amount of results obtained from *in vitro* cell response and from clinical tests on implant surfaces [6, 9]. However, not all rough surfaces appear to possess the same capability to promote the expression of a mature osteoblastic phenotype *in vitro* and to facilitate bone formation *in vivo*. Furthermore there is an increasing awareness that rough surfaces frequently face the issue of peri-implantitis, a serious condition that often leads to implant failure. In this context, titanium surface topography has been shown to play a pivotal role in disease prevention and possibly progression [6].

In the present work, we showed the responses of murine osteoblasts on machined and commercially available rough titanium surfaces, to further investigate their physicochemical characteristics, the pattern of protein adsorption on both surfaces and cell morphological and proliferative responses [10]. We showed that surface treatment affected titanium wettability, consistently with the literature [11] but did not appear to significantly modify its surface chemical composition. We have to consider that the contact angle measurement is slightly influenced by surfaces roughness [12], but we can assume that this aspect is negligible for our purposes. Most interestingly however, the pattern of protein adsorption was quite different between machined and ZirTi® surfaces and protein adsorption is known to be affected by surface physicochemical characteristics, including wettability [13].

Proteins spontaneously adsorb on surfaces by creating weak molecular bonds, e.g. van der Waals, dipoles or hydrogen interactions, according to complex molecular models. Hydrophilic or hydrophobic protein domains can differently interact with biomaterial surfaces, and this may lead to changes in protein conformation upon adsorption [14], and therefore their activity. Thus, investigating protein adsorption can provide interesting insights into subsequent cell behaviours. Although the method we used in the present study does not allow to precisely label the protein species that are affected, machined surfaces seem to adsorb higher amounts of proteins (fig.3.5), including a 150 kDa peptide and an approximately 60 kDa peptide. However, some protein species, like some relatively light peptides in the range from 25 to 15 kDa were detectable only on ZirTi® surfaces. It is possible to thus conclude that the pattern of protein adsorption seems to differ between the two tested groups, although for most detected protein species machined surfaces seem to bind higher amounts of peptides. This may at least in part explain why cell viability was increased on machined samples at Calcein assay. Actually, it has been reported that the quality of proteins adsorption on titanium surfaces plays a pivotal role in subsequent cell adhesion [14]. Similarly, proliferation on smoother samples was higher than on rough discs already after 48 hours of culture and even more at later time-points (fig.3.8), although the absence of mechanical hurdles on machined discs may also have facilitated the faster duplication of cells. However, our studies did not reveal a closer adhesion of osteoblasts to machined surfaces than to the ZirTis®, suggesting that titanium microtopography did not alter cell attachment (fig.3.9C-D). Cytofluorescence analysis confirmed these data by revealing a comparable expression of vinculin in cells cultured on machined surfaces

and on ZirTi® (fig.3.9 A-B), and thus of focal adhesions, the multiprotein complexes that are responsible for anchoring cells to the underlying substrate. Our gene expression data confirmed that osteoblastic cells on rough ZirTi® surfaces expressed higher levels of differentiation markers over time, including ALP, OPG, OPN and OCN. Interestingly mRNA levels for CKD1, a gene that is involved in cell cycle progression tended to be more highly expressed on Machined surfaces by day 7, consistently with our cell viability observations (fig.3.7 and fig.3.8). Taken together, our data show that machined and ZirTi® titanium surfaces have a different protein adsorption pattern, differently affect cell proliferation and differentiation, with Machined surfaces supporting faster cell growth and ZiTi surfaces promoting a more mature osteoblastic phenotype.

Bibliography

[1] Le Guéhennec L, Soueidan A, Layrolle P, Amouriq Y. *Surface treatments of titanium dental implants for rapid osseointegration.* Dent Mater 2007; 23: 844–854.

[2] Anselme K. *Osteoblast adhesion on biomaterials.* Biomat 2000 21:667-681.

[3] Albrektsson T, Wennerberg A. *Oral implant surfaces: part 1. Review focusing on topographic and chemical properties of different surfaces and in vivo responses to them.* Int J Prosthodont 2004; 17: 536–543.

[4] Schwartz Z, Martin J Y, Dean D D, Simpson J, Cochran D L, Boyan B D. *Effect of titanium surface roughness on chondrocyte proliferation, matrix production, and differentiation depends on the state of cell maturation.* J Biomed Mater Res 1996; 30: 145–155.

[5] Passeri G, Cacchioli A, Ravanetti F, Galli C, Elezi E, Macaluso GM. *Adhesion pattern and growth of primary human osteoblastic cells on five commercially available titanium surfaces.* Clin Oral Impl Res 2010; 21:756-765.

[6] Junker R, Dimakis A, Thoneick M, Jansen J A. *Effects of implant surface coatings and composition on bone integration: a systematic review.* Clin Oral Implants Res 2009; 20(Suppl 4): 185–206.

[7] Esposito M, Coulthard P, Thomsen P, Worthington HV. *The role of implant surface modifications, shape and material on the success of osseointegrated dental implants. A Cochrane systematic review.* Eur J Prosthodont Restor Dent. 2005 Mar;13(1):15-31.

[8] Barbour ME, Dominic JO, Jenkinson HF, Jagger DC. *The effects of polishing methods on surface morphology, roughness and bacterial*

colonization of titanium abutments. J Mater Sci Mater Med 2007; 18:1439-1447.

[9] Jayraman M, Meyer U, Bühner M, Joos U, Wiesmann HP. *Influence of titanium surfaces on attachment of osteoblast-like cells in vitro.* Biomaterials 2004; 25 (4):625-631.

[10] Banik BL, Riley TR, Platt CJ, Brown JL. *Human mesenchymal stem cell morphology and migration on microtextured titanium.* Front Bioeng Biotechnol. 2016; 10:4-41.

[11] Morra M, Cassinelli C, Bruzzone G, Carpi A, Di Santi G, Giardino R, Fini M. *Surface chemistry effects of topographic modification of titanium dental implant surfaces: 1. Surface analysis.* Int J Oral Maxillofac Implants. 2003 Jan-Feb;18(1):40-5.

[12] Rupp F, Gittens RA, Scheideler L, Marmur A, Boyan BD, Schwartz Z, Geis-Gerstorfer J. *A review on the wettability of dental implant surfaces I: theoretical and experimental aspetcs.* Acta Biomaterialia 2014; 10:2894-2906.

[13] Kopf BS, Ruch S, Berner S, Spencer ND, Maniura-Weber K. 2015. *The role of nanostructures and hydrophilicity in osseointegration: In-vitro protein-adsorption and blood-interaction studies.* J Biomed Mater Res Part A 2015:103A:2661–2672.

[14] Gittens RA, Scheideler L, Rupp F, Hyzy SL, Geis-Gerstorfer J, Schwartz Z, Boyan BD. *A review on the wettability of dental implant surfaces II: Biological and clinical aspects.* Acta Biomaterialia 2014; 10:2907–2918.

Chapter 4

Surfaces characterization

4.1 Introduction

Titanium has been recognized for more than 40 years to be a safe and effective therapeutic option in implant dentistry. Indeed, titanium is a suitable biomaterial to produce dental implants used as root replacement for the anchorage of prostheses, crowns or bridges [1]. After its placement, dental implant come directly in contact with the surrounding biological seal and many aspects of its surface can modify the performance, consequently influencing osseointegration, including surface micro topography, chemical composition and wettability. According to literature, the surface energy of an implant, which is related to implant wettability, is nowadays considered a peculiar characteristic that affect the biological response of the milieu to the implant [2, 3], and studies have been published on the improved performances of hydrophilic surfaces [4, 5, 6].

As a consequence, in recent years, research and dental implants productors faced the challenge of obtaining high wettable titanium surfaces. In literature different ways to obtain super hydrophilic titanium surfaces are described. Zhao and Buser pioneered the field at the beginning of the twenty-first century, combining the storage

in physiological saline solution and gamma-ray irradiation to preserve titanium surface wettability and to prevent its biological aging [7, 8]. Few years later Aita and Hori proposed to apply the mechanism of photocatalisis to obtain hyper hydrophilic titanium surfaces [9, 10] while Ueno et al. used a gamma-ray treatment in order to remove organic contaminants and consequently to improve titanium hydrophilicity [11]. Considered the benefits guaranteed by high wettable dental implant surfaces and the efforts in the research of methods to obtain and maintain titanium super-hydrophilicity, we were able to develop a new method to improve surface wettability. The proprietary method to obtain super hydrophilic surfaces was developed both for smooth and rough titanium implants. However, we will not describe the fully procedure followed to obtain these modified surfaces because the treatment is currently under patent application.

Once obtained high wettable surfaces, we wanted to investigate how our treatment influences any changement in chemical, morphological, physical and biochemical characteristics of the surfaces; aspects that determine the biological cascade of events at the interface with the surrounding milieu, and the consequent implant osseointegration. In particular, we deeply investigated protein adsorption to observe how the differences in this process could influence subsequent cell adhesion. In general, it has been shown that wettability influence the bonding strength, the amount, the conformation and the orientation of proteins at the interface [12]. However, nobody has already investigated if hydrophilicity influences the selectivity of titanium for specific proteins essential for biological responses such as cell adhesion or bone tissue healing in the subsequent phases after implant placement. For that, in this chapter we want to further highlight the

role of wettability in enhancing surface selectivity for different blood proteins, with particular regards to fibronectin, a protein which plays a key role in cell adhesion, and to fibrinogen, one of the major actor in healing processes.

The method was tested on ZirTi® and machined surfaces whose respective role in terms of protein adsorption, cell proliferation, viability and adhesion was tested as shown in Chapter 2.

4.2 Materials and methods

4.2.1 Titanium discs

Commercially pure, grade 4 (ISO5832/2) titanium discs with a diameter of 8.0mm and a thickness of 3.5mm were used for properties characterization. The discs were supplied by Sweden&Martina S.P.A. (Due Carrare, Padova, Italy). Half of the discs were machined and not treated at the end of the milling process, while other half were acid-etched and sandblasted following the procedure used by Sweden&Martina to obtain ZirTi® implant surface. All titanium discs were cleaned in an Argon-activated plasma reactor and sterilized, following the procedure used for Sweden&Martina commercialy available implants.

4.2.2 Surface treatment

A new method to enhance titanium surfaces hydrophilicity was developed, even though it can not be declared because it is actually under patent application.

Both machined and ZirTi® discs were divided into two groups: one used as control and one treated according to our method. Consequently the disks were divided in 4 groups:

- MC: Machined Hydrophobic Titanium Discs;
- MT: Machined Hydrophilic Titanium Discs;
- ZC: ZirTi® Hydrophobic Titanium Discs;
- ZT: ZirTi® Hydrophilic Titanium Discs.

4.2.3 Physical characterization

Surface differences in hydrophilicity were assessed by the measurement of the contact angle on hydrophilic and not titanium surfaces. Five µl of water were deposited on machined and ZirTi® discs using a pipette and the contact angle with the surface was measured on standardized photographs through ImageJ software (ImageJ, U. S. National Institutes of Health, Bethesda, MD, USA). Figure 4.1 schematically represent three different levels of surface wettability measured through the contact angle between a water droplet and the surface.

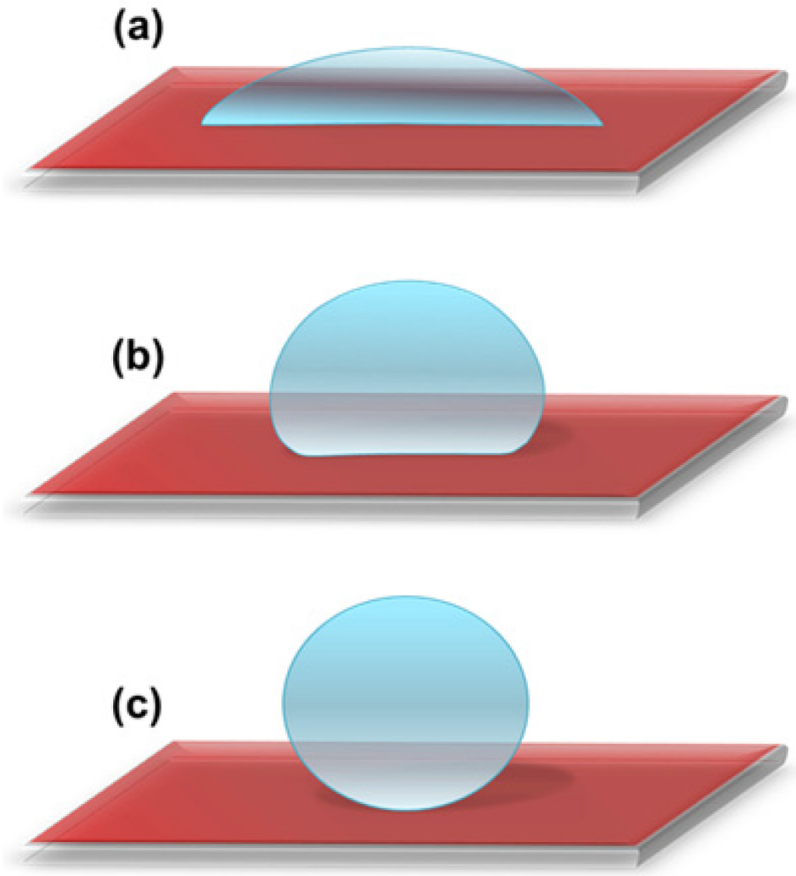

FIGURE 4.1: Different levels of surface wettability measured through the contact angle of a water droplet: hydrophilic surface (A), moderately hydrophobic surface (B) and completely hydrophobic surface (C).

4.2.4 Chemical characterization

To investigate differences in titanium surfaces chemistry, a Raman spectroscopy, combined with X-Ray photoelectron spectroscopy (XPS) was developed.

Raman Spectroscopy

Raman spectroscopy is a spectroscopic technique used to observe vibrational, rotational, and other low-frequency modes in a system. Raman spectroscopy is commonly used in chemistry to provide a fingerprint by which molecules can be identified. It relies on inelastic scattering, or Raman scattering, of monochromatic light, usually from a laser in the visible, near infrared or ultraviolet range. The laser light interacts with molecular vibrations and photons, resulting in the energy of the laser photons being shifted up or down. The shift in energy gives information about the vibrational modes in the system. Infrared spectroscopy yields similar, but complementary, information.

Raman spectroscopy was used to provide fingerprints of the surfaces, by which molecules can be identified. Non-polarized Raman spectra were recorded at 632.8 nm (nominal 15 mW He–Ne laser excitation) in a nearly backscattered geometry with a Jobin Yvon LabRAM micro-spectrometer (300 mm focal length spectrograph) equipped with an integrated Olympus BX40 microscope provided with x10, x50 and x100 objectives. The resolution of the spectra was assessed between 1.5–2 cm^{-1}. The Rayleigh radiation was blocked by an edge filter and the backscattered Raman light was dispersed by a 1,800-groove mm^1 holographic grating on a Peltier cooled CCD, consisting of an array of 1024x256 pixels. The entrance slit width was fixed

at 100µm. The laser power was maintained less of 3mW. Spectra were collected using both 100 and long working distance 50 microscope objectives. Typical exposures were 10–60 s repeated three to five times. The system was regularly calibrated using the 520.6 cm^1 Raman band of silicon or by means of reference emission lines of Ar or Cd light sources. The data analysis was performed by LabSpec built-in software.

X-Ray Photoelectron Spectroscopy (XPS)

X-ray photoelectron spectroscopy (XPS) is a surface-sensitive quantitative spectroscopic technique that measures the elemental composition at the parts per thousand range, empirical formula, chemical state and electronic state of the elements that exist within a material. XPS spectra are obtained by irradiating a material with a beam of X-rays while simultaneously measuring the kinetic energy and number of electrons that escape from the top 0 to 10 nm of the material being analyzed. The XPS characterization apparatus includes an X-ray source with photon Mgka (1253.6eV) with resolution depending on the pass energy values (PE) set [13].

XPS analysis was performed to determine the chemical and electronic state of the elements on the surfaces. XPS was performed ex situ in a UHV apparatus, using the Mg-K emission at 1253.6 eV as x-ray photon source. Photoelectrons were analyzed by a VSW HA100 electron energy analyzer, leading to a total energy resolution of 0.86 eV. Core level binding energies (BE) were referred to the Au 4f7/2 core level signal (at 84.0 eV), obtained from a sputtered gold surface. The photoemission core levels of all elements were analyzed through Voight lineshape deconvolution, after background subtraction of a

Shirley function. The typical precision for energy peak position was 0.05eV, while uncertainty for full width at half-maximum (FWHM) was less than $\pm$ 5%, and $\pm$ 5% for area evaluation.

4.2.5 Morphology

To investigate whether any difference in surface topographical aspect of titanium surfaces, a scanning electron microscopy analysis (SEM) was done. Hydrophobic and hydrophilic, machined or ZirTi®, titanium discs were sputtered with a thin layer of gold through a SCD 040 coating device (Balzer Union, Wallruf, Germany) and observed using a dual beam Zeiss Auriga Compact system equipped with a GEMINI Field-Effect SEM column (Zeiss, Oberkochen, Germany). The analysis was performed at 5keV.

4.2.6 Protein adsorption

To study adsorption of serum proteins to titanium surfaces, a quantitative and qualitative protein analysis was performed. For quantitative analysis, titanium discs were soaked in a 200µg/ml BSA or fibronectin solution for 2 hours. Protein concentration in supernatants was measured after 5, 15, 30, 60, 120 and 180 minutes through the Bradford (BIO-RAD Protein Assay, BIO-RAD, Hercules, CA, USA). Briefly, aliquots of 10µl were mixed with 200µl of Bradford Working Solution and incubated at 37°C for 2 minutes. Finally, sample absorbances were read at 620nm with a Multiskan FC plate reader (Thermo Fisher Scientific, Waltham, MA, USA). For qualitative analysis, titanium discs were incubated in 500µl of Phosphate Buffered Saline (PBS, Sigma-Aldrich, Italy) in the presence of 2% Human Serum (HS from human male AB plasma, Sigma-Aldrich) for 1 hour at room

temperature (RT). The discs were then rinsed twice in PBS to remove unbound proteins and covered with 80µl of Sample Buffer 1X (Tris-HCl 62.5mM pH 6.8, SDS 1.5%w/v, DTT 100mM, with traces of Bromophenol Blue). Complete recovering of bound proteins was obtained freezing, thawing, sonicating for 15 minutes, and boiling the discs for 10 minutes. Equal volumes of the protein samples were then loaded on 12% polyacrylamide gel (Acrylamide/Bis-Acrylamide 30%, Sigma-Aldrich) and separated at 180V for 1 hour. After running, the gel was exposed to Comassie solution (Comassie Brilliant Blue, Bio-Rad, USA) for protein staining. For Western Blot analysis, separated plasma proteins were blotted on PVDF membrane (Immobilon-P, Darmstadt, Germany) at 100V for 1h. Non-specific binding sites were blocked with an incubation in Tris-buffer saline (TBS; 50 mM Tris–HCl, pH 7.5, 150 mM NaCl) containing 10% of blocking reagent (Roche SpA, Italy) for 1h at RT. Membranes were then incubated with anti-Fibrinogen (Abcam, UK), anti-Fibronectin (Sigma-Aldrich), anti-transferrin (Abcam), anti-ceruloplasmine (Abcam), anti-albumin (Cell Signaling Technology, MA; USA) primary antibodies diluted 1:800 in TBS 0.1% Tween 20 supplemented with 5% BSA. After washing, membranes were incubated with HRP-conjugated secondary antibody diluted 1:10000 (Cell Signaling Technology, MA, USA). Finally, immunoreactivity was visualized with enhanced chemiluminescence (Immobilon Western Chemiluminescent HRP, Millipore).

4.2.7 Statistical analysis

Data were analyzed using Prism 6 (GraphPad, La Jolla, CA, USA). All values are reported as the mean $\pm$ SD of three repeated experiments. Differences between group means were evaluated with two-way ANOVA statistical tests with Tukey post-test and differences were considered significant when $p<0.05$.

4.3 Results

4.3.1 Titanium physical properties

The treatment we used induces an evident gain of titanium hydrophilicity. Figure 4.6 shows the results of contact angle measurement. The differences in hydrophilicity between control and treated surfaces were statistically different both for the machined and for the ZirTi®. However, even though the machined control surface (fig.4.2) was more hydrophilic than the ZirTi® control surface (fig.4.4), ZirTi® gain of hydrophilicity was more marked than that of the machined surface and the ZirTi® treated surface (fig.4.5) resulted more hydrophilic than the machined treated surface (fig.4.3).

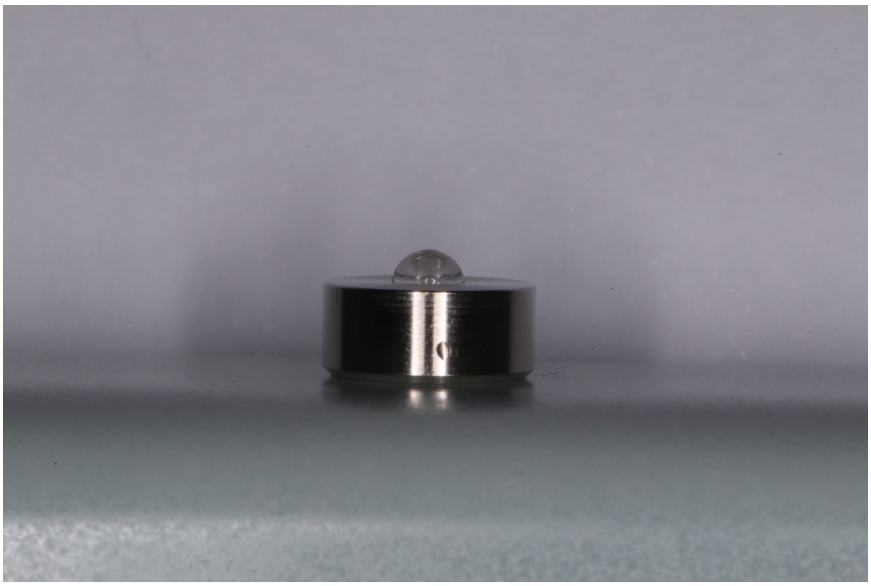

FIGURE 4.2: Standardized photograph of a control machined surface showing the contact angle with a 5µl drop of water.

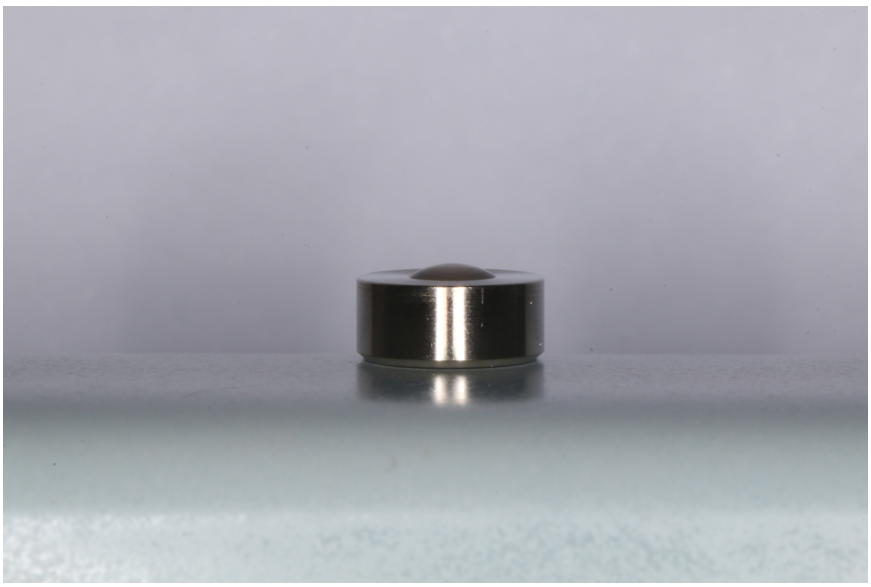

FIGURE 4.3: Standardized photograph of a treated machined surface showing the contact angle with a 5µl drop of water.

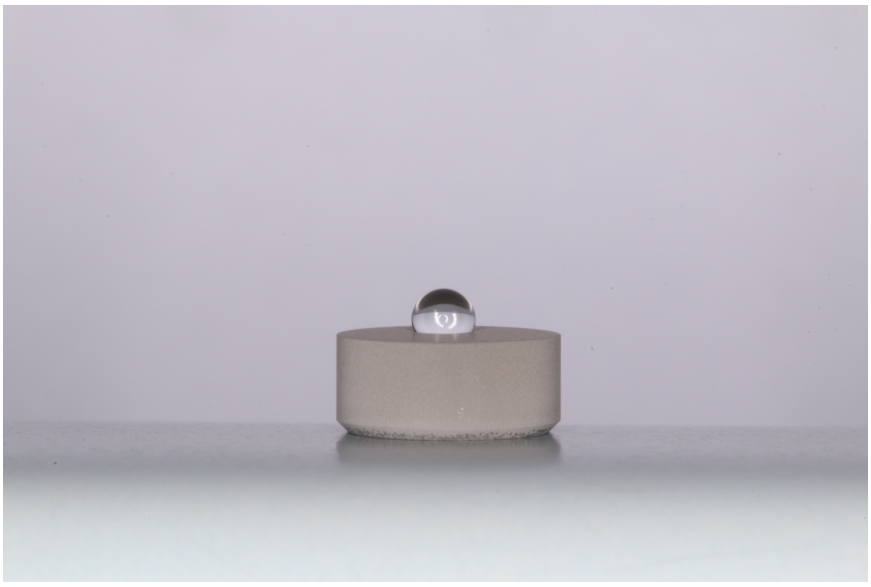

FIGURE 4.4: Standardized photograph of a control ZirTi® surface showing the contact angle with a 5µl drop of water.

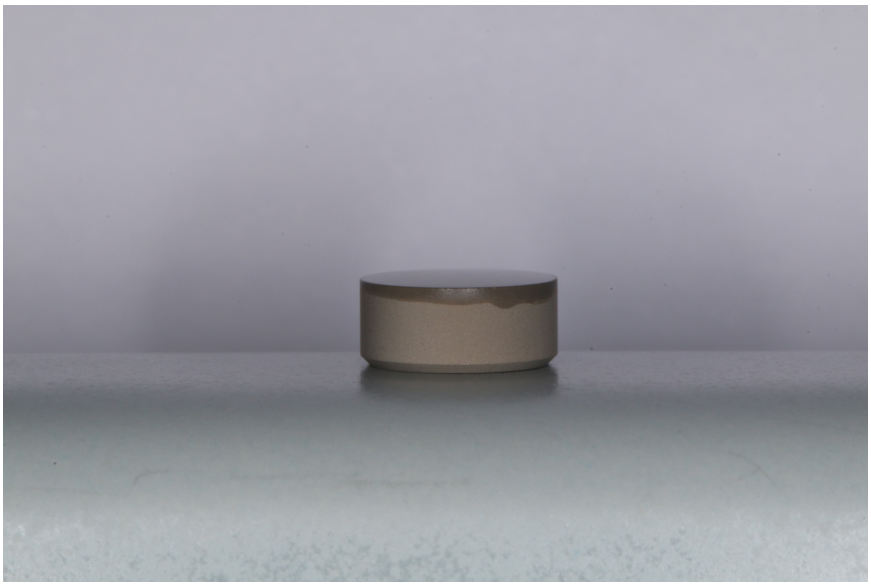

FIGURE 4.5: Standardized photograph of a treated ZirTi® surface showing the contact angle with a 5µl drop of water.

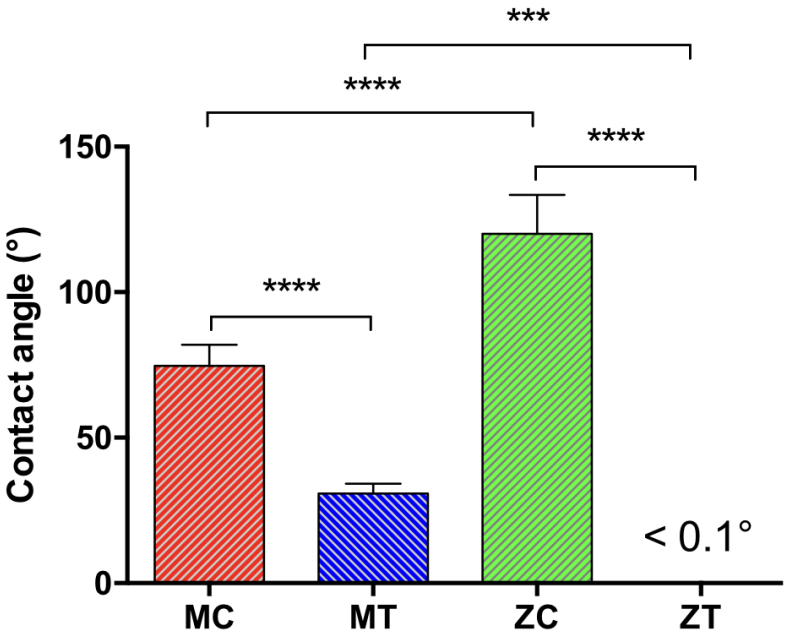

FIGURE 4.6: Histograms representing contact angle between titanium surface and water droplet, before and after the treatment. ***=p<0.002; ****=p<0.001.

4.3.2 Titanium chemical properties

X-Ray Photoelectron Spectroscopy (XPS)

XPS investigation revealed that the main chemical species were oxygen, titanium and carbon, as shown in the wide range spectra reported in figure 4.7.

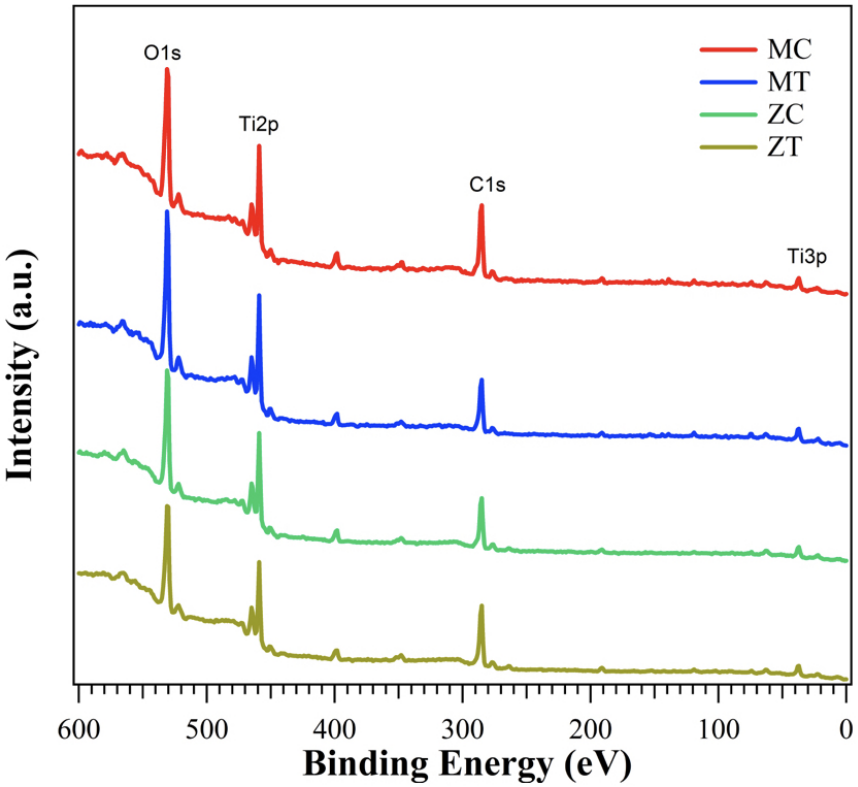

FIGURE 4.7: XPS wide range spectrum of the machined and ZirTi® samples.

Moreover, other minor contributes, in their oxidized chemical states, could be identified in a BE region between 30 and 150 eV. The chemical composition of all the samples in terms of surface atomic percentage is summarized in figure 4.8.

Core level spectra of titanium (Ti2p) and oxygen (O1s) are reported in figure 4.9A and figure 4.9B, respectively. Titanium Ti2p core level was characterized by two main structures placed to a distance of 5.7 eV, as expected from the spin-orbit splitting of the 2p

	MC	MT	ZC	ZT
other	9.88	11.39	9.46	8.07
% O	35.97	40.00	37.24	34.04
% C	44.68	37.63	42.26	48.64
% Ti	9.47	10.98	11.04	9.25

FIGURE 4.8: Atomic percentage of all the chemical species present in the samples.

peaks.

From a chemical point of view, titanium was present in form of TiO_2 (Ti^{4+}) at 459.20 eV [13], with a small contribution from Ti_2O_3, located at lower binding energy (457.80 eV). The respective energy position, the percentage with regard to the total Ti2p area and the atomic percentage are reported in figure 4.10.

O1s core level analysis was more complex, due to the presence of six components correlated with all the oxide species of carbon, titanium, magnesium, aluminum, silicon and lead (fig.4.9B). Main peaks at 530.80 eV refer to oxygen in TiO_2 (blue component), while different species from Al_2O_3 and MgO and PbOx could not be resolved and gave rise to component at 530.60eV (light green component). Other components were present, related to C-O and C=O carbonyl groups at 532.25eV (red component) and hydroxyl groups on the titanium oxide at 533.20eV (pink component), as well as other minor contributions coming from silicon oxides at 532.10eV (dark green component)

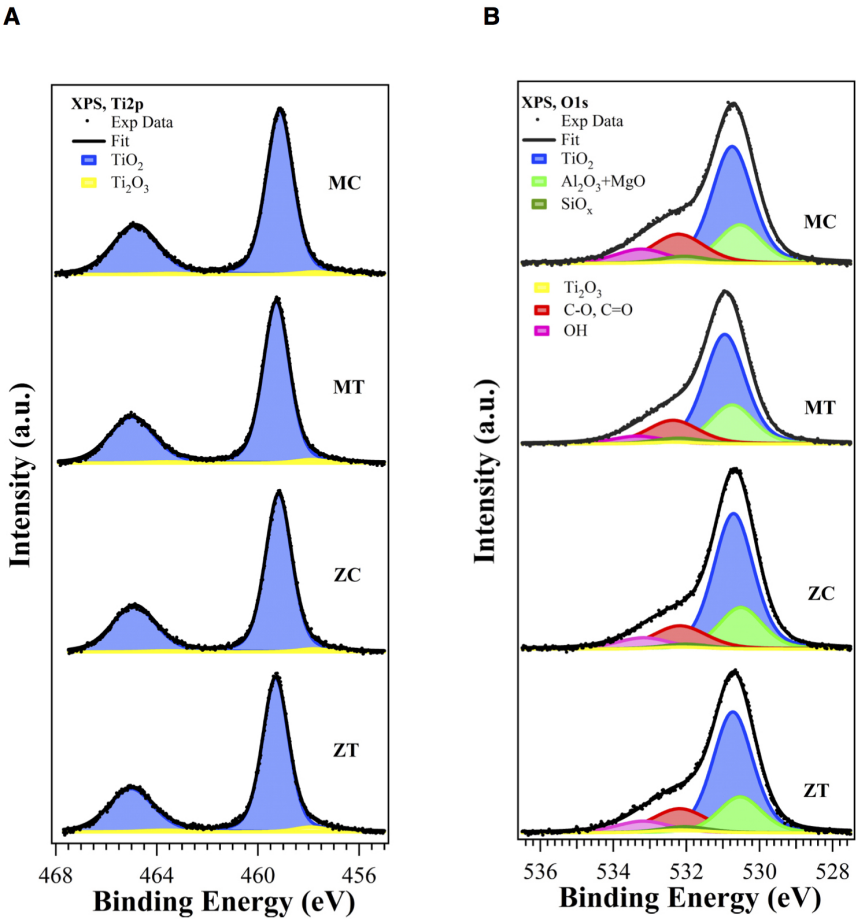

FIGURE 4.9: XPS core level spectra (background subtracted). (A) Ti2p core level and (B) O1s core level.

and Ti_2O_3 at 532.20eV (yellow component). A complete description of all components is reported in figures 4.11 and 4.12.

O1s Core Level	MC			MT			ZC			ZT		
	BE [eV]	%	Atom %	BE [eV]	%	Atom %	BE [eV]	%	Atom %	BE [eV]	%	Atom %
TiO_2	530.75	46.20	16.60	530.95	50.20	20.00	530.71	53.20	19.80	530.73	50.20	17.10
Ti_2O_3	532.19	0.80	0.30	532.38	1.10	0.40	532.14	1.10	0.40	532.16	1.60	0.60
C-O C=O	532.22	21.60	7.70	532.40	18.50	7.40	532.18	17.10	6.30	532.19	19.60	6.70
OH	533.23	11.90	4.20	533.34	8.20	3.30	533.17	8.70	3.20	533.18	9.40	3.00
Metal Oxide	530.54 532.06	19.50	7.00	530.75 532.21	22.00	8.80	530.51 532.02	19.90	7.40	530.53 532.04	19.20	6.60

FIGURE 4.10: Analysis of O1s core level of all the samples.

Ti2p Core Level	MC			MT			ZC			ZT		
	BE [eV]		%	BE [eV]		%	BE [eV]		%	BE [eV]		%
	2p 3/2	2p 1/2		2p 3/2	2p 1/2		2p 3/2	2p 1/2		2p 3/2	2p 1/2	
Ti4+ (TiO_2)	459.13	464.85	98.10	459.28	465.00	97.40	459.18	464.90	97.70	459.30	465.00	96.10
Ti3+ (Ti_2O_3)	457.73	463.45	1.90	457.87	463.59	2.60	457.78	463.50	2.30	457.90	463.62	3.90

FIGURE 4.11: Analysis of Ti2p core level of all the samples.

	MC	MT	ZC	ZT
Ti4+ (TiO_2)	9.30	10.70	10.80	8.90
Ti3+ (Ti_2O_3)	0.20	0.30	0.20	0.40

FIGURE 4.12: Atomic percentage of the TiO2 and Ti2O3 species in the samples.

Raman Spectroscopy

Raman Spectroscopy did not show significant modifications of the fingerprints of the surfaces. Crystal form of titanium dioxide were not found on any surface.

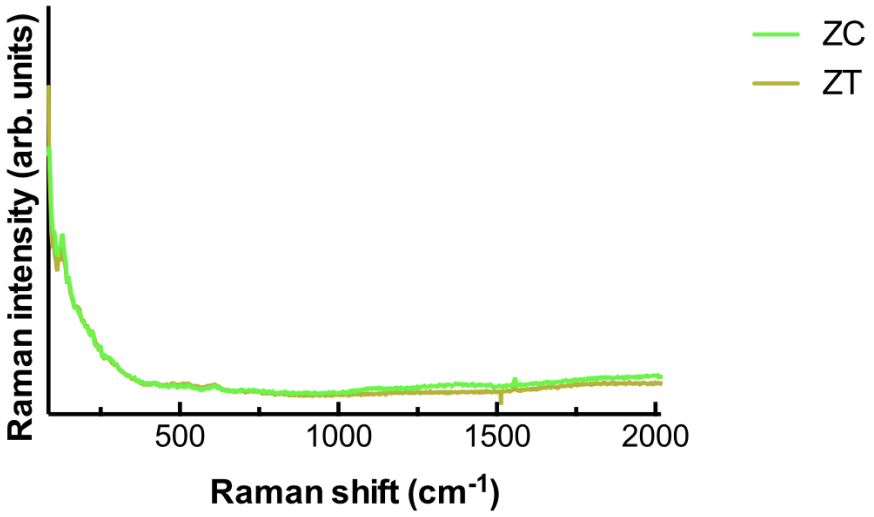

FIGURE 4.13: Typical Raman spectra of ZirTi® surfaces.

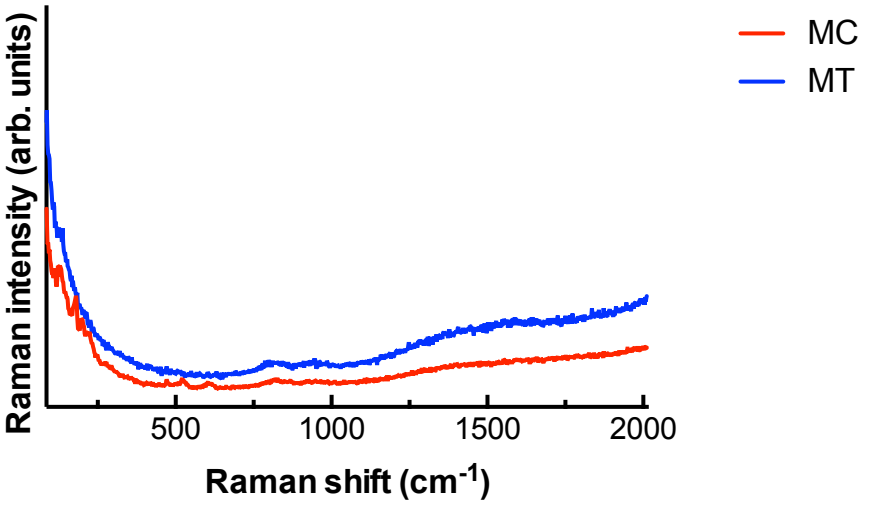

FIGURE 4.14: Typical Raman spectra of machined surfaces.

4.3.3 Titanium morphological properties

Our treatment did not alter topographical aspect of titanium. SEM investigation revealed that the morphological aspect of the surfaces were not subjected to any modification after the treatment. Figure 4.15 shows the typical microscopical aspects of the surfaces.

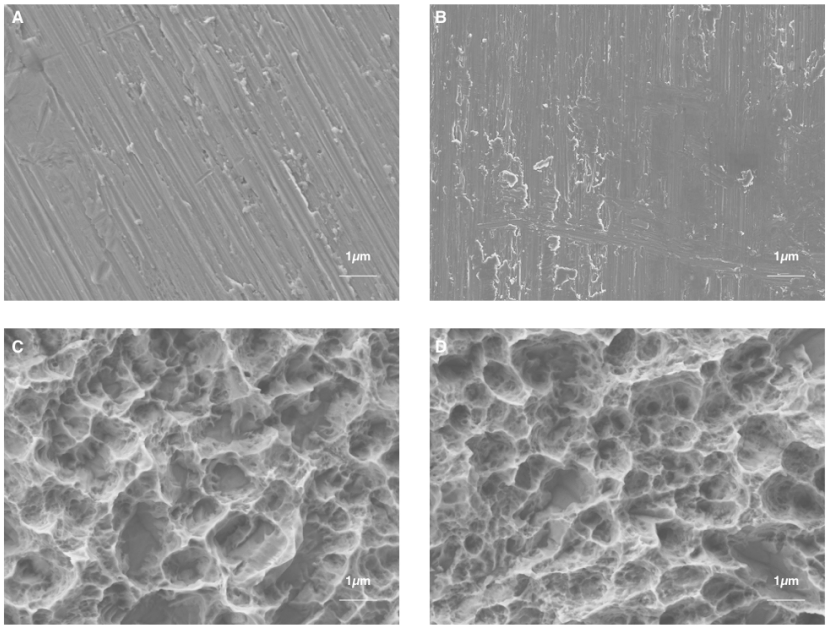

FIGURE 4.15: Typical SEM images of machined hydrophobic (A) or hydrophilic (B), and of ZirTi® hydrophobic (C) or hydrophilic (D) titanium surfaces microtopography.

4.3.4 Protein adsorption

Our treatment did not influence quantitative protein adsorption phenomena. To investigate whether hydrophilicity influence the amount of adsorbed proteins a Bradford assay for BSA (fig.4.16, 4.18) and for fibronectin (fig.4.17, 4.19) was developed. Hydrophilicity did not alter the amount of proteins adsorbed on the surfaces, and the amount of total protein adsorbed was comparable between all the surfaces. MC adsorbed a mean of 12.53 $\pm$ 0.26 µg of BSA and 13.63 $\pm$ 0.66 µg of fibronectin. MT adsorbed a mean of 13.12 $\pm$ 0.10 µg of BSA and 13.87 $\pm$ 1.39 µg of fibronectin. ZC adsorbed a mean of 13.75 $\pm$ 0.02 µg of BSA and 12.33 4$\pm$ 2.50 µg of fibronectin. ZT adsorbed a mean of 14.07 $\pm$ 0.11 µg of BSA and 13.87 $\pm$ 1.39 µg of fibronectin.

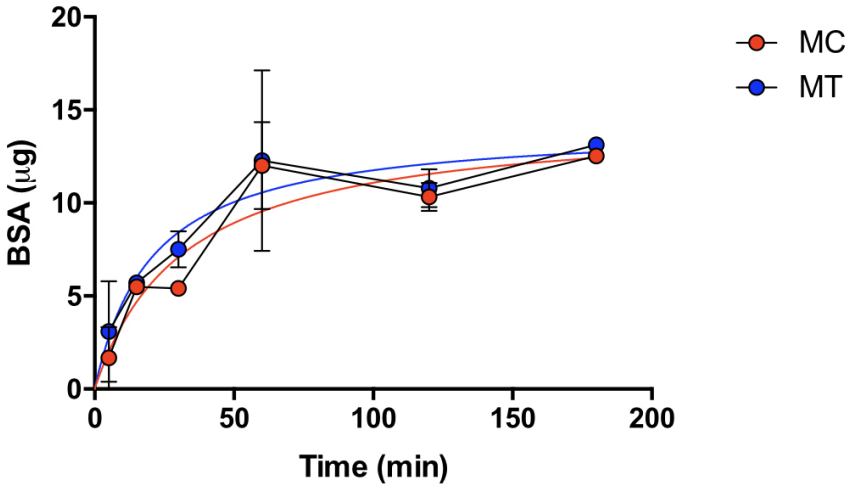

FIGURE 4.16: Curves representing albumine adsorption on machined titanium surfaces over time.

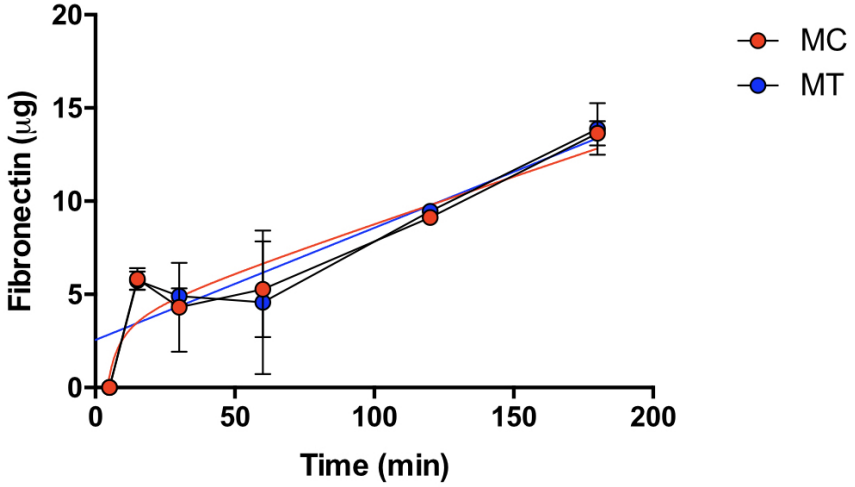

FIGURE 4.17: Curves representing fibronectin adsorption on machined titanium surfaces over time.

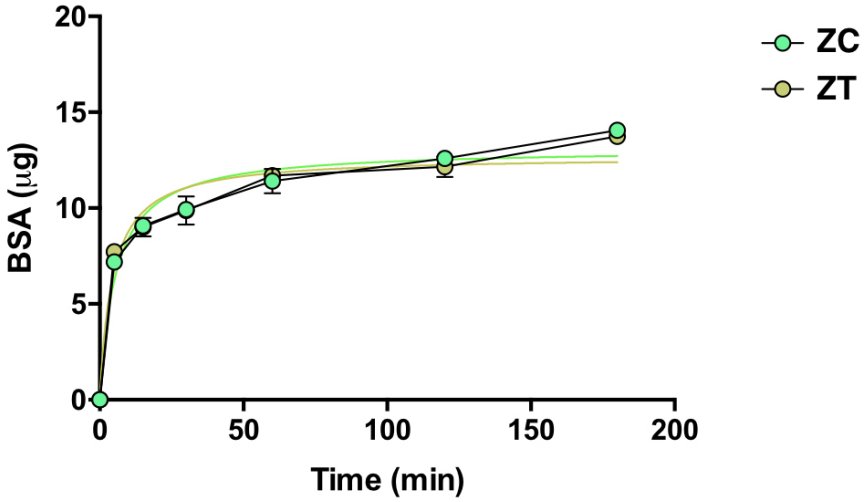

FIGURE 4.18: Curves representing albumine adsorption on ZirTi® titanium surfaces over time.

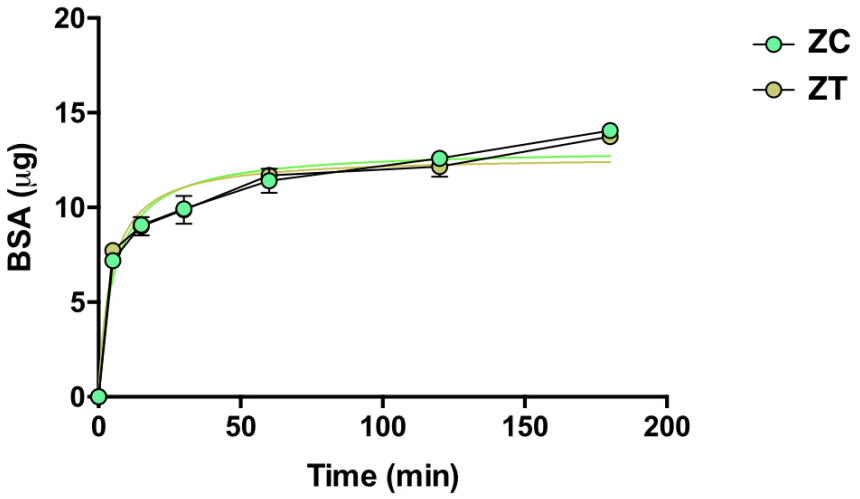

FIGURE 4.19: Curves representing fibronectin adsorption on ZirTi® titanium surfaces over time.

Figure 4.20 reports the characterization of adsorbed serum proteins by machined and ZirTi® titanium discs. Untreated machined discs adsorbed more serum proteins then ZirTi® counterparts (fig.4.20, lane MC vs. lane ZC). Interestingly, our treatment enhanced the adsorption capacity of both titanium preparations. To preliminarily characterize the identity of proteins adsorbed by the different discs, before and after the treatment, a series of Western blots was performed to assess the binding of some representative serum proteins, such as fibrinogen (FG), fibronectin (FBN), transferrin (TF) and albumin (ALB). FG and FBN were the most evidently adsorbed serum proteins by both types of titanium discs. The adsorption pattern was different for the different proteins. Indeed, while FBN was more largely adsorbed by machined than ZirTi® discs (fig.4.22, lanes MC vs lane ZC), the reverse was observed for FG (fig.4.21), lanes MC vs lane ZC). After the treatment, a roughly proportional increase of adsorbed FBN and FG was observed on both titanium surfaces (Fig.4.22), lanes MC and MT vs ZC and ZT, respectively). As far as the other serum proteins are concerned, TF was adsorbed more by untreated machined than ZirTi® discs (fig.4.23, lanes MC vs. ZC), a pattern even more evident for albumin (fig.4.24). For TF and ALB, the treatment produced a significant increase in adsorption to ZirTi® discs, but not to machined discs. CP adsorption (not shown) exhibited only minor differences among the different materials.

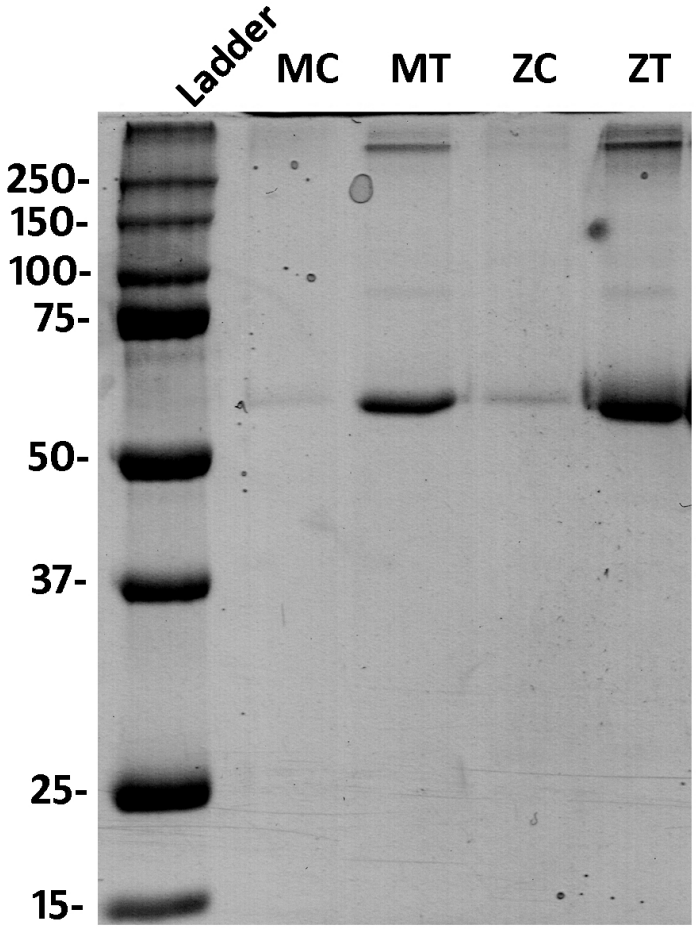

FIGURE 4.20: 10% SDS-PAGE of protein adsorbed on machined and ZirTi® titanium surfaces.

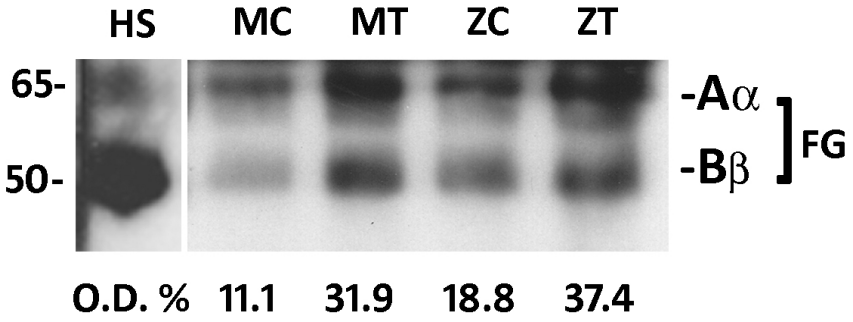

FIGURE 4.21: Western Blot analysis of fibrinogen adsorption on machined and ZirTi® titanium surfaces. Under each line, the relative quantification of the adsorbed protein, derived from the densitometric analysis, is shown.

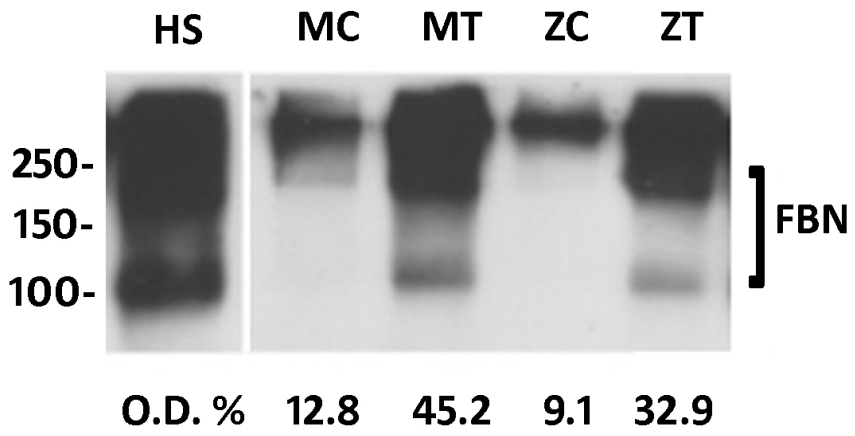

FIGURE 4.22: Western Blot analysis of fibronectin adsorption on machined and ZirTi® titanium surfaces. Under each line, the relative quantification of the adsorbed protein, derived from the densitometric analysis, is shown.

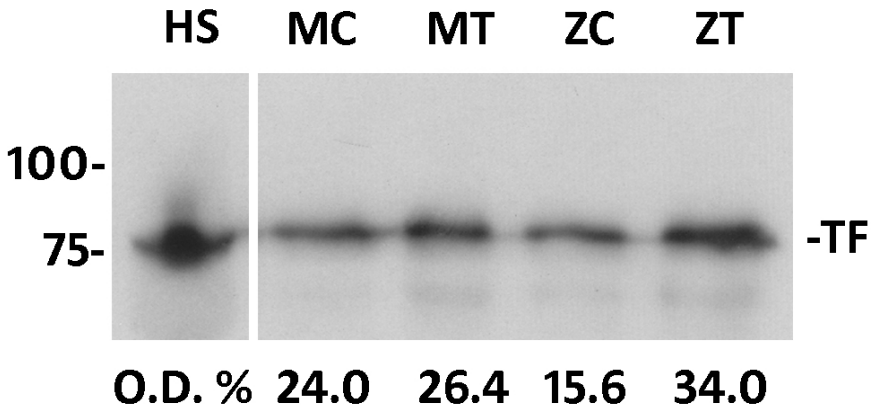

FIGURE 4.23: Western Blot analysis of transferrin adsorption on machined and ZirTi® titanium surfaces. Under each line, the relative quantification of the adsorbed protein, derived from the densitometric analysis, is shown.

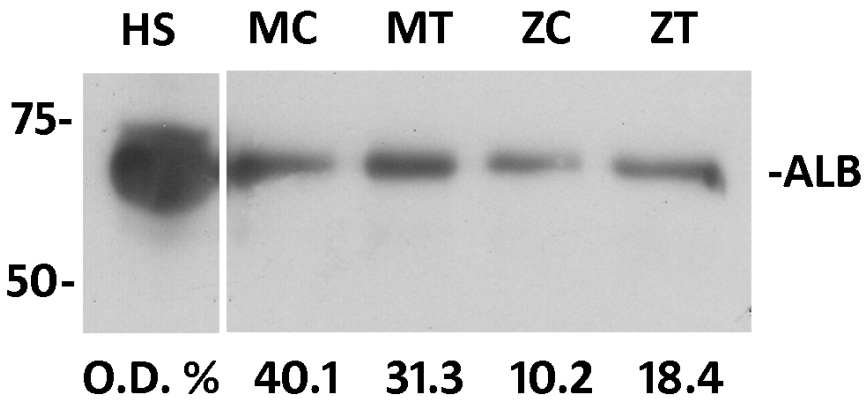

FIGURE 4.24: Western Blot analysis of albumine adsorption on machined and ZirTi® titanium surfaces. Under each line, the relative quantification of the adsorbed protein, derived from the densitometric analysis, is shown.

4.4 Discussion

The surface energy of an implant, measured through the liquid-solid contact angle and related to surface wettability, is one of the characteristics which affect the biological response of an implant [14]. In literature, many surface modifications have been proposed in order to increase the wettability of the surfaces [15], however no methods have been already found to obtain surface without modification in chemical and morphological aspects. Here we proposed to obtain hydrophilic surfaces through the use of a property method, which do not induce any modification of titanium surfaces. The method we proposed induce a substantial gain of surface wettability, without alter other characteristics of the material. As reported in figures 4.4, 4.5 and 4.6, the treatment induce a dramatic augmentation of ZirTi® surface wettability, which from an hydrophobic state passes to a super hydrophilic state (fig.4.4, 4.5, 4.6), while a moderate one of the machined, which from an hydrophobic state passes to a hydrophilic state (fig.4.2, 4.3, 4.6). To observe any eventual chemical changement of the surface, an XPS was combined to a Raman Spectroscopy analysis. XPS analysis performed on all samples proves the presence of three predominant elements, carbon, oxygen and titanium, with other minor species, which contribute can not be eluded, being the 9.88% for the MC, the 11.39% for the MT, the 9.46% for the ZC and the 8.07% for the ZT of the total composition (fig.4.8). These chemical species are all oxidized, as demonstrated by the analysis of the O1s core level. The lineshape deconvolution puts in evidence that their contribution represents the 7% of the total oxygen signal (fig.4.10). Moreover, their intensity increases after the treatment on the machined samples, whereas it remains unchanged in the ZirTi®

(fig.4.10). The BE position of Ti2p peaks indicate that the titanium is completely oxidized in the TiO_2 and Ti_2O3 forms [13], without any traces of the metallic form. More in detail, it seems that, apparently, the treatment induces a small increment of both the oxidized species TiO_2 and Ti_2O_3 in all the machined samples and in ZC. The ZT sample shows, instead, a reduction of the TiO_2 intensity after the treatment.

According to XPS analysis, Raman spectroscopy did not reveal any changement in fingerprints of the surfaces both for the machined and the ZirTi® samples (fig.4.10). Morphological differences were investigate too through a SEM analysis, and did not revealed any changement in the topographical aspect of ZirTi® and machined titanium surfaces (fig.4.15). According to the literature, hydrophobic and hydrophilic titanium surfaces should adsorb the same amount of proteins, but hydrophilicity should influence the bonding strength, conformation and macromolecular film composition of adsorbed proteins [12, 14]. In our analysis we showed that the adsorption of albumin and fibronectin is comparable on both hydrophilic and hydrophobic, machined or ZirTi®, titanium surfaces (fig.4.22, 4.24). Moreover, we can observe that albumin and fibronectin seem to be adsorbed on the surfaces accordingly to the Vroman effect: albumine is massively adsorbed within 60 minutes on the samples (fig.4.20, 4.22), stabilizing subsequently at a plateau, while fibronectin seems to be constantly adsorbed over the time, overpassing the amount of albumine adsorbed after 180 minutes (fig.4.21, 4.23) [16]. The Vroman effect justifies also the patterning of adsorption shown by Western blot analysis, which revealed that albumin, fibrinogen and fibronectin are increasingly adsorbed after 1 hour of incubation in 2%

human serum solution. Concerning the amount of adsorbed proteins, we can observe that, after the washing of titanium discs into PBS, treated surfaces retained more proteins than untreated samples (fig.4.20). Concerning the composition of macromolecular films, hydrophilicity seems to highly influence the type of proteins adsorbed on the surface. Fibronectin (fig.4.22), fibrinogen (fig.4.21) and albumin (fig.4.24) seem to be adsorbed according to Vroman effect, but moreover the hydrophilic surfaces lead to the bonding of more fibrinogen and fibronectin. The amount of Fibrinogen was significatively higher on treated surfaces than on untreated ones (fig.4.21); from the literature we know that fibrinogen is involved in the inflammatory response and a major amount of fibrinogen could be connected to faster tissue reparation. Considering our aim, a massive adsorption of fibrinogen may be useful to enhance titanium osseointegration in vivo. On the other hand, a marked adsorption of fibronectin is evident (fig.4.22). Fibronectin is one of the proteins majorly involved in cell adhesion and in scaffold colonization [17, 18] and its massive adsorption is essential for a better adhesion of osteoblasts, as we will show in the second part of this work, and for a supposed rapid osseointegration of the implant. Concerning albumin (fig.4.24) and transferrin (fig.4.23), no significative differences were observed and this indicates that our treatment leads to an amelioration in selectivity of the surfaces for specific proteins.

Taken together, our results demonstrate that the treatment we used to modify the wettability of commercially available titanium surfaces, lead to an amelioration in biochemical characteristics of the implants, whithout altering their morphological and chemical aspects. The amelioration in protein adsoprtion is essential in the

light of a faster osseintegration phenomenon and it reflects a better cells response*in vitro*, as we will show in the following chapter of this work.

Bibliography

[1] Branemark PI, Hansson BO, Adell R, Breine U, Lindstrom J, Hallen O, et al. *Osseointegrated implants in the treatment of the edentulous jaw. Experience from a 10-year period.* Scand J Plast Reconstr Surg Suppl 1977;16:1-132.

[2] Massaro C, Rotolo P, DE Riccardis F, Milella E, Napoli A, Wieland M. *Comparative investigation of the surface properties of commercial titanium dental implants. Part I. Chemical composition.* J Mater Sci Mater Med 2002;13:535-48.

[3] Le Guehennec L, Soueidan A, Layrolle P, Amouriq Y. *Surface treatments of titanium dental implants for rapid osseointegration.* Dent Mater 2007;23:844-54.

[4] Eriksson C, Nygren H, Ohlson K. *Implantation of hydrophilic and hydrophobic titanium discs in rat tibia: cellular reactions on the surfaces during the first 3 weeks in bone.* Biomaterials 2004;25:4759-66.

[5] Bornstein MM, Valderrama P, Jones AA, Wilson TG, Seibl R, Cochran DL. *Bone apposition around two different sandblasted and acid-etched titanium implant surfaces: a histomorphometric study in canine mandibles.* Clin Oral Implants Res 2008;19:233-41.

[6] Rupp F, Gittens RA, Scheideler L, Marmur A, Boyan BD, Schwartz Z, Geins-Gerstorfer J. *A review on the gettability of dental implant surfaces I: Theoretical and experimental aspects.* Acta Biomater 2014;10(7):2894-906.

[7] Zhao G, Schwartz Z, Wieland M, Rupp F, Geis-Gerstorfer J, Cochran DL *High surface energy enhances cell response to titanium substrate microstructure.* J Biomed Mater Res 2005;74A:49–58.

[8] Buser D, Broggini N, Wieland M, Schenk RK, Denzer AJ, Cochran DL, et al. *Enhanced bone apposition to a chemically modified SLA titanium surface.* J Dent Res 2004 83:529-533.

[9] Aita H, Hori N, Takeuchi M, Suzuki T, Yamada M, Anpo M, Ogawa T. *The effect of ultraviolet functionalization of titanium on integration with bone.* Biomaterials. 2009;30(6):1015–1025.

[10] Hori N, Ueno T, Suzuki T, Yamada M, Att W. *Ultraviolet light treatment for the restoration of aged-related degradation of titanium bioactivity.* Int J Oral Maxillofac Implants 2010;25:49–62.

[11] Ueno T, Takeuchi M, Hori N, Iwasa F, Minamikawa H, Igarashi Y, et al. *Gamma ray treatment enhances bioactivity and osseointegration capability of titanium.* J Biomed Mater Res B Appl Biomater 2012 100:2279-2287.

[12] Andrade JD, Hlady V. *Protein adsorption and materials biocompatibility - a tutorial review and suggested hypotheses.* Adv Polum Sci 1986;79:1-63.

[13] Chastainand RCK. *Handbook of X-ray photoelectron spectroscopy*. Physical Electronics, Inc., 1992, USA.

[14] Gittens RA, Scheideler L, Rupp F, Hyzy SL, Geis-Gerstorfer J, Schwartz Z, Boyan BD. *A review on the wettability of dental implant surfaces II: Biological and clinical aspects.* Acta Biomaterialia 10 (2014) 2907–2918.

[15] Junker R, Dimakis A, Thoneick M, Jansen JA. *Effects of implant surface coatings and composition on bone integration: a systematic review.* Clin Oral Implants Res 2009;20(Suppl4):185-206.

[16] Vroman L, Adams Al, Fischer GC, Munoz PC. *Interaction of high molecular weight kininogen, factor XII, and fibrinogen in plasma at interfaces.* Blood 1980;55(1):156-9.

[17] Allouni ZE, Gjerdet NR, Cimpan MR, Hoi PJ. *The effect of blood protein adsorption on cellular uptake of anatase TiO2 nanoparticles.* Int J Nanomedicine 2015;10:687-95.

[18] Lima EMCX, Koo H, Vacca-Smith AM, Rosalen PL, Del Bel Cury AA. *Adsorption of salivary and serum proteins, and bacterial adherence on titanium and zirconia ceramic surfaces.* Clin Oral Impl Res 2008;19:780-85.

Chapter 5

Investigation of MC3T3-E1 cells behaviour on the surfaces

5.1 Introduction

Accordingly to the worldwide accepted definition of biocompatibility, an implant is considered biocompatible when it performs into the biological niche where it is inserted, and when it induces an appropriate response of the tissue concerning its specific application [1]. Titanium is considered a suitable biomaterial to produce dental implants, which have been recognized for more than 40 years to be a safe and effective options in implantology [2]. The optimal osseointegration of an implant is a parameter that influences its biocompatibility, and several studies have shown that osseointegration is seriously influenced by titanium surface aspects, included microtopography, chemical composition and wettability [3]. With particular regard to wettability, research is nowadays deeply focused on its amelioration, and many efforts have been done to find methods fo ameliorate it [4, 5, 6]. One major point, that induce researchers to focus on surface wettability is its ability of guiding the quality of protein adsorption at the interface. In fact, when an implant is positioned, proteins are massively adsorbed on the surface, theoretically

without being altered in term of conformation and function, either a bad cell adhesion could occur [7]. Accordingly to Gittens et al. [8], titanium hydrophilic surfaces allow protein adsorption as well as titanium commercially available in term of the amount of protein adsorbed, although hydrophilic surfaces lead to the preservation of protein conformation at the interface, inducing a better adsorption in term of quality. Considering this, hydrophilic titanium surfaces should enhance the biocompatibility of titanium in term of cell adhesion and proliferation. According to this, we applied the method characterized in Chapter 4, which is able to enhance titanium surfaces wettability without altering chemical and morphological composition of the surface. In fact, in the previous chapter, we demonstrated that our treatment induces a dramatic gain of wettability of titanium surface, as well as it allows a correct protein adsorption, also ameliorating the selectivity of our surfaces for fibronectin, a protein majorly involved in cell adhesion. After having chemically, physically, morphologically and biochemically characterized hydrophilic and hydrophobic, machined or ZirTi® titanium surfaces in the previous chapter, we wanted to investigate the ability of hydrophilic and hydrophobic, machined or ZirTi® titanium surfaces, to differently enhance cell adhesion, proliferation and differentiation, in order to ameliorate osseointegration of titanium dental implants.

5.2 Materials and methods

Commercially pure, grade 4 (ISO5832/2) titanium discs with a diameter of 8.0mm and a thickness of 3.5mm were used for properties characterization. The discs were supplied by Sweden&Martina S.P.A. (Due Carrare, Padova, Italy). Half of the discs were machined and not treated at the end of the milling process, while other half were acid-etched and sandblasted following the procedure used by Sweden&Martina to obtain ZirTi® implant surface. All titanium discs were cleaned in an Argon-activated plasma reactor and sterilized, following the procedure used for Sweden&Martina commercialy available implants.

Both machined and ZirTi® discs were divided into two groups: one used as control and one treated according to our method. Consequently the disks were divided in 4 groups:

- MC: Machined Hydrophobic Titanium Discs;
- MT: Machined Hydrophilic Titanium Discs;
- ZC: ZirTi® Hydrophobic Titanium Discs;
- ZT: ZirTi® Hydrophilic Titanium Discs.

5.2.1 *In vitro* assays

Cell culture

In vitro assays were all performed with murine osteoblasts (MC3T3-E1) obtained from the American Type Culture Collection (LGC Standards, S.R.L., Sesto S.Giovanni, MI, Italy). Cells were cultured in complete Alpha-MEM (Alpha-MEM, Life Technologies, Carlsbad, CA;

USA) addicted with 10% Fetal Bovine Serum (FBS, Life Technologies) and 1% Penicillin and Streptomycin (Penstrep, Sigma Aldrich). After 72 hours of culture complete medium was enriched with ascorbic acid 250µM (Sigma-Aldrich). Tests were all performed in 48-well plates (JET BIOFIL, Guangzhou, China) by positioning titanium discs on the bottom of the well and seeding above the cells at a density of 10000 cells/disc.

Live/dead Assay

To investigate the influence of hydrophilicity on cell viability, cells were stained with Calcein AM, Propidium Iodide (PI) and DAPI for LIVE/DEAD assay. After 48 hours of culture, culturing medium was removed and cells were stained for 10 minutes at room temperature (RT) in dark conditions with a 4µM Calcein AM (Calcein AM, LifeTechnologies), 7.5µM PI (PI, LifeTechnologies) and 5µg/ml DAPI solution (DAPI, LifeTechnologies) in Phosphate Buffer Saline (PBS, Sigma-Aldrich). Samples were then fixed with a 4% paraformaldheyde solution (PFA, Sigma-Aldrich) for 20 minutes in dark conditions and observed with a stereomicroscope equipped for fluorescence (SMZ25, Nikon, Tokyo, Japan). Three range of interest areas (ROI) were chosen and viable and dead cells were counted through the use of the Documentation software (Documentation D3, Nikon).

Metabolic activiy assay

To observe the influence of hydrophilicity on cell metabolic activity, a Resazurin Sodium Salt assay was developed. Twenty-four, 48, and 72 hour after seeding 100µl of the Resazurin Sodium Salt stock solution (final concentration 0.15mg/ml) were added every 500µl of serum-free culturing medium and samples were incubated at 37°C and 5%

CO2 for 4 hours. Fluorescence was exited at 560nm and emitted at 585nm by a Multiskan Ascent microcell plate reader (Thermo Labsystems, Helsinki, Finland).

Cell adhesion

To investigate whether hydrophilicity influences the rate of cell adhesion to surfaces, a trend curve for adhesion was designed. Five, 15, 30 minutes, 1, 3, 6 and 24 hours after seeding titanium discs were turned upside down in the culturing well and cells which not adhered to surfaces were left to fall in the culturing medium for 2 minutes by gravity as shown in figure 5.1. Cells adhered to surfaces were subsequently quantitated by chemiluminescence assay (CellTiterGLO, Promega, Milan, Italy) following manufacture's recommendations. Briefly, samples were incubated with 200µl of a 50:50 solution of culturing medium and Lysis Buffer for 2 minutes on a shaker. Luminescence was stabilized in dark conditions for 10 minutes and finally assessed with the luminometer (GLO-MAX 20/20, Promega).

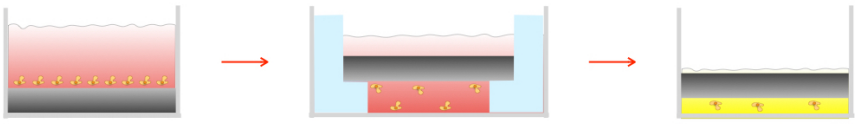

FIGURE 5.1: Diagram representing the method used to design the adhesion trend line of cells to hydrophobic and hydrophilic surfaces. Cells were seeded on titanium discs, which at the desired time point were turned upside down and cells adhered were quantitated trough the chemiluminescence.

Cytofluorescence

To observe focal adhesion expression a cytofluorescence was performed for focal adhesion, cytoskeleton and cell nuclei. After 24 hour of culture, culturing medium was removed and cells were fixed in 4% PFA solution for 10 minutes at RT. After two rinses in PBS, cells were permeabilized with 0.1% v/v Triton X-100 (Sigma-Aldrich) for 5 minutes at RT and washed twice with the PBS. One-% Bovine Serum Albumine solution (BSA, Sigma-Aldrich) was applied for 30 minutes at RT. Cells were subsequently treated with a primary anti-Vinculin monoclonal antibody, clone 7F9 (FAK100, Merck Millipore, Darmstadt, Germany), for focal adhesion staining (1:100 dilution) for 1 hour at RT and subsequently washed twice in PBS. To reveal the primary antibody, a secondary anti-rabbit antibody labeled with the AlexaFluor®488 (LifeTechnologies) (dilution 1:200) was co-incubated with TRITC-conjugated phalloidin (FAK100, Merck Millipore) (dilution 1:200) for actin staining. After three washes with PBS, nuclear counterstaining was performed by sample incubation with DAPI (FAK100, Merck Millipore). Sample images were taken with a stereomicroscope equipped for fluorescence (SMZ25, Nikon). Three representative range of interest areas (ROI) were chosen and focal adhesion per cell were counted through the use of the Documentation software (Documentation D3, Nikon).

Cell morphology

A scanning electron microscopy (SEM) was performed in combination with the orthogonal cutting of cells through a Gallium Focused Ion Beam (FIB) source, to study cells morphology and their interactions with the underlying titanium disc at the interface. SEM-FIB preparation was completely performed at RT 24 hours after seeding.

At the end of the culture, culturing medium was removed and cells were rinsed in PBS (Sigma-Aldrich). Subsequently, cells were fixed in a 2.5% glutaraldehyde solution (Sigma-Aldrich) in Na-Cacodylate buffer solution (Sigma-Aldrich) for 30 minutes, washed in Na-Cacodylate buffer (Sigma-Aldrich) for 5 minutes, and dehydrated in ethanol at increasing concentration (Sigma-Aldrich). Finally, samples were critical point dried with the liquid carbon dioxide (CPD 030 Baltec, Wallruf, Germany) and sputtered with a thin layer of gold though a SCD 040 coating device (Balzer Union, Wallruf, Germany). Sample microphotographs were taken using a dual beam Zeiss Auriga Compact system equipped with a GEMINI Field-Effect SEM column and a Gallium Focused Ion Beam (FIB) source (Zeiss, Oberkochen, Germany). The SEM analysis was performed at 5 keV, while the cross-sectional analysis with FIB was performed accelerating Gallium ion beam at 30kV with a current of 10pA.

5.2.2 Statistical analysis

Data were analyzed using Prism 6 (GraphPad, La Jolla, CA; USA). All the values are reported as the mean $\pm$ SD of three repeated experiments. Differences between groups were evaluated with the two-way ANOVA statistical test with Bonferroni's multiple comparisons post-test and differences were considered significant when $p<0.05$.

5.3 Results

5.3.1 Cell viability and proliferation

To study whether hydrophilicity of implant surfaces could influence cell viability, activity and proliferation, MC3T3-E1 cells were seeded on treated and control machined or ZirTi® titanium discs and assayed through LIVE/DEAD, Resazurin Sodium salt assay.
LIVE/DEAD assay fig.5.2 A,B,C,D) showed higher cell viability both on the control and on the treated sample, as well as on machined and on ZirTi® surface. Few dead cells were detectable and differences between the number of live and of dead cells were significative on both the surfaces (fig.5.3, 5.4). However, treated machined titanium surface seems to severe influence cell proliferation, and more osteoblasts were counted on the treated sample than on the control (fig.5.3). On the other hand, the difference between the number of live cells on the control and on the treated sample is no significative on ZirTi® surface (fig.5.4).

On the other hand, Resazurin sodium salt assay showed no difference in cell metabolism on both the surfaces, hydrophilic or hydrophobic (Fig. 5.5, 5.6).

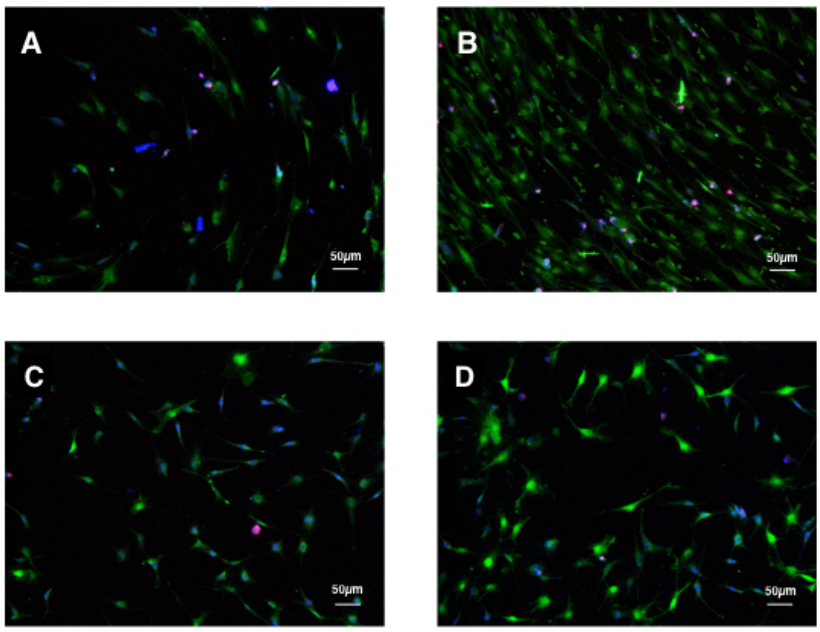

FIGURE 5.2: Microphotographs showing MC3T3-E1 cells on hydrophobic (A) and hydrophilic (B) machined titanium surfaces and on hydrophobic (C) and hydrophilic (D) ZirTi® surfaces after Calcein AM, PI and DAPI staining. Microphotographs showing MC3T3-E1 cells on hydrophobic (D) and hydrophilic (E) ZirTi® titanium surfaces after Calcein AM, PI and DAPI staining.

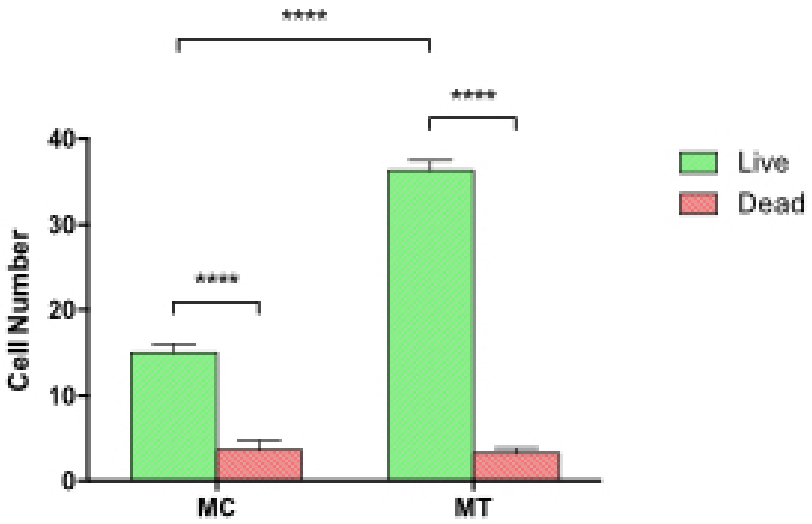

FIGURE 5.3: Histograms showing the mean of viable and dead cells on machined surfaces. * = p<0.05; ****=p<0.001.

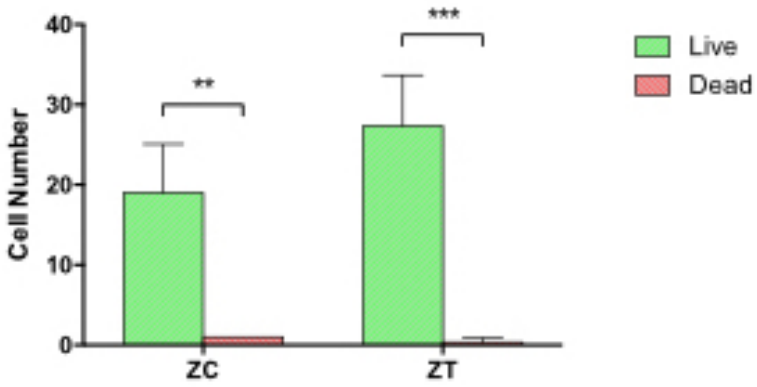

FIGURE 5.4: Histograms showing the mean of viable and dead cells on ZirTi® surfaces. * = p<0.05; ****=p<0.001.

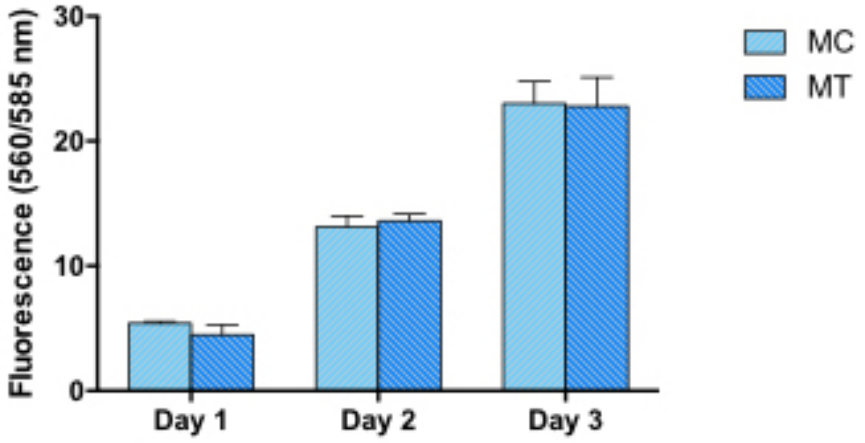

FIGURE 5.5: Histograms showing MC3T3-E1 cells metabolic activity assessed through the Resazurin Sodium salt assay on machined titanium surfaces 24, 48 and 72 hours after seeding.

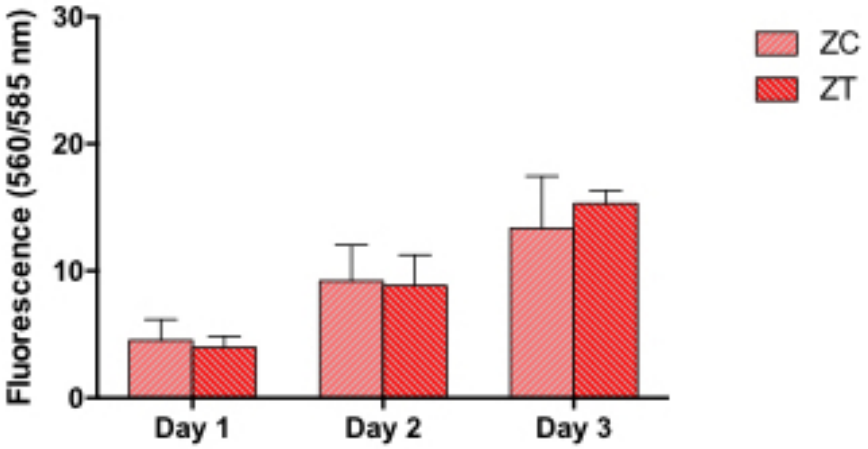

FIGURE 5.6: Histograms showing MC3T3-E1 cells metabolic activity assessed through the Resazurin Sodium salt assay on ZirTi® titanium surfaces 24, 48 and 72 hours after seeding.

5.3.2 Cell adhesion and morphology

To investigate the role of hydrophilicity on cell adhesion, MC3T3-E1 cells were seeded on treated and control machined or ZirTi® titanium discs and were analyzed through chemiluminescence, cytofluorescence and SEM-FIB analysis. Chemiluminesce assay was used to quantify the number of adhered cells to the surface 5, 15, 30 minutes, 1, 3, 6 and 24 hours after seeding and to design a trend line of cell adhesion to titanium (fig.5.7, 5.8).

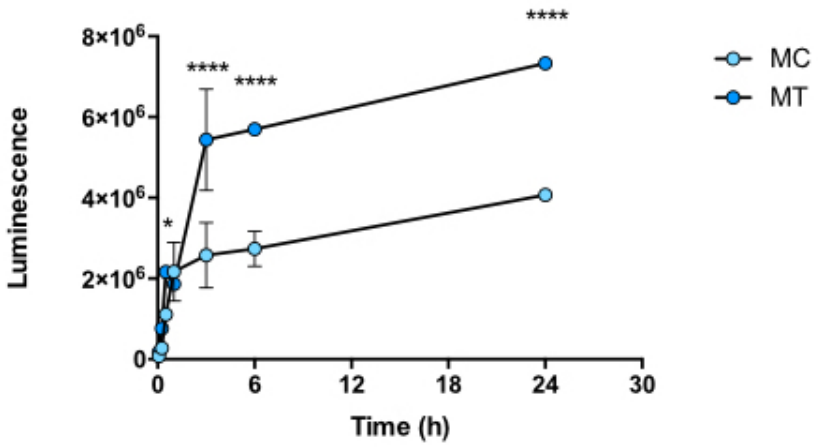

FIGURE 5.7: Evolution curves representing MC3T3-E1 cells speed of adhesion to machined surfaces. * = p<0.05; ****=p<0.001.

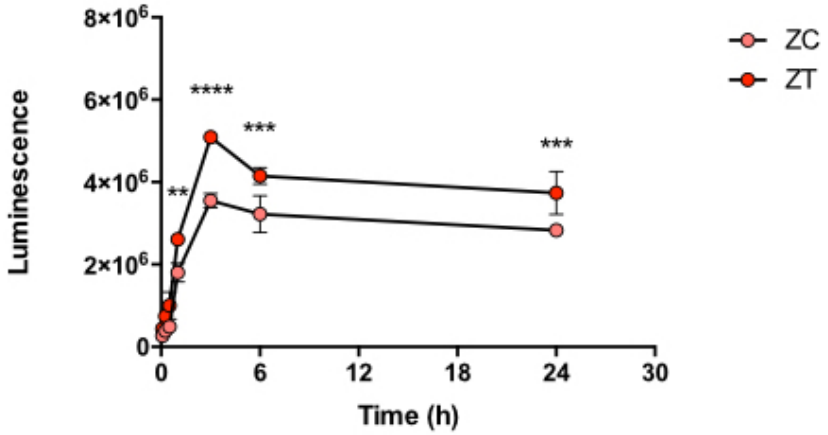

FIGURE 5.8: Evolution curves representing MC3T3-E1 cells speed of adhesion to ZirTi® titanium surfaces. * = p<0.05; ****=p<0.001.

The number of adhered cells increase along the time. After 5, 15 and 30 minutes more cells were adhered to the hydrophilic surfaces both on the machined and on the ZirTi® surfaces, but with no significative differences. However, already after 1 hour the differences between the groups were statistically different and the number of attached cells was stable in a plateau until 24 hours.

To confirm the data obtained with the chemiluminescence assay, a SEM-FIB analysis was developed in order to study cell morphology and their way of adhesion to the substrates. Figure 5.9 reports typical SEM images of MC3T3-E1 cells on hydrophilic and hydrophobic machined or ZirTi® titanium surfaces 24 hours after seeding. Considering machined surfaces (fig.5.9A-F), cells before seem to adhere equally on the control and on the treated sample, showing a flat shape. Different cell behavior was observed on ZirTi® surfaces. Figure 5.9G-L reports typical SEM images of MC3T3-E1 cells on hydrophilic and hydrophobic ZirTi® titanium surfaces 24 hours after seeding. Already before FIB cuts, cells on treated sample seems to adhere better to the surfaces, showing a flatter shape, which lead to glimpse the morphology of ZirTi® surface under cell bodies. On the other hand cells on the control show a less attached cell soma. FIB analysis confirm SEM observations, ZirTi® hydrophilic surfaces promote a closer adhesion of osteoblasts, cells adhere preferentially to surface peaks and seems to be thinner.

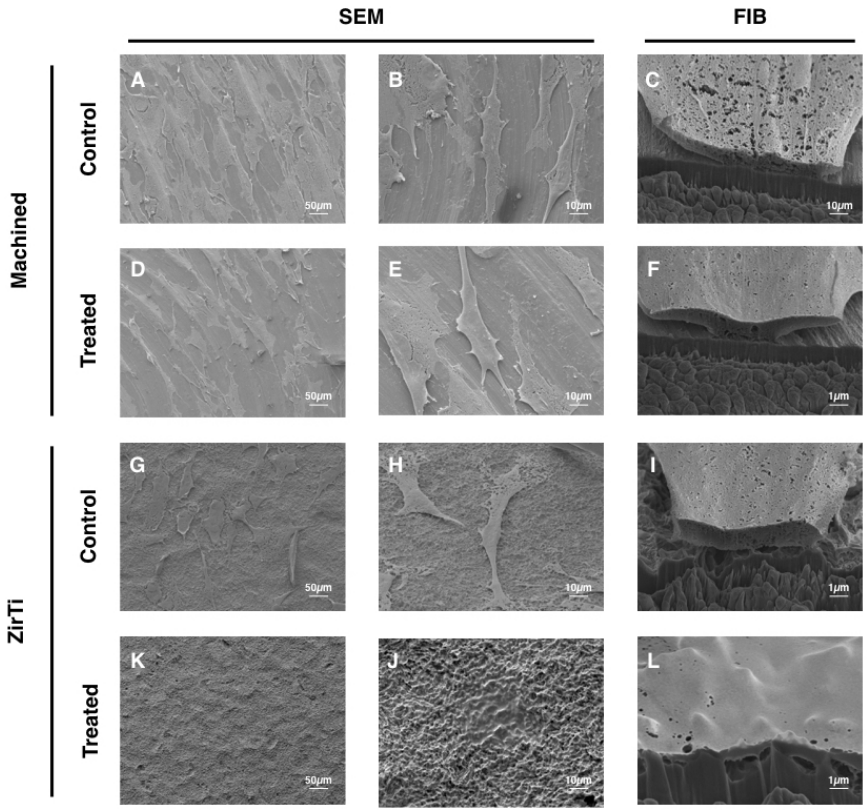

FIGURE 5.9: Typical SEM images of MC3T3-E1 cells cultured on hydrophilic and hydrophobic machined or ZirTi® titanium surfaces after 24 hours of culture (A, B, D, E, G, H, K, J). SEM images of MC3T3-E1 cells cultured on hydrophilic and hydrophobic machined or ZirTi® titanium surfaces and cut with a FIB source (C, F, I, L).

Cytofluorescence for focal adhesion after 24 hours (fig.5.10) confirm datas of SEM-FIB analysis. More focal adhesion were observed on treated sample than on the control, after the staining for vinculin (green spots), and the differences between the groups are significative (fig. 5.11, 5.12). However, focal adhesion seems to be higher expressed on machined discs than on the ZirTi®, highlighting the importance of surface morphology in cell adhesion.

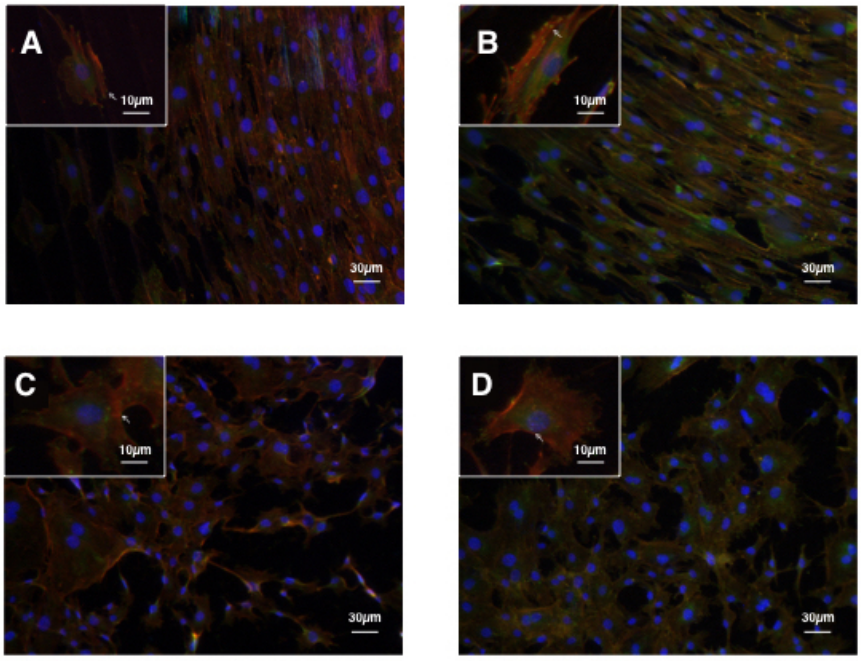

FIGURE 5.10: Microphotographs showing MC3T3-E1 cells on hydrophobic (A) and hydrophilic (B) machined titanium surfaces and on hydrophobic (C) and hydrophilic (D) after actin (red), vinculin (green spots) and DAPI (blue) staining.

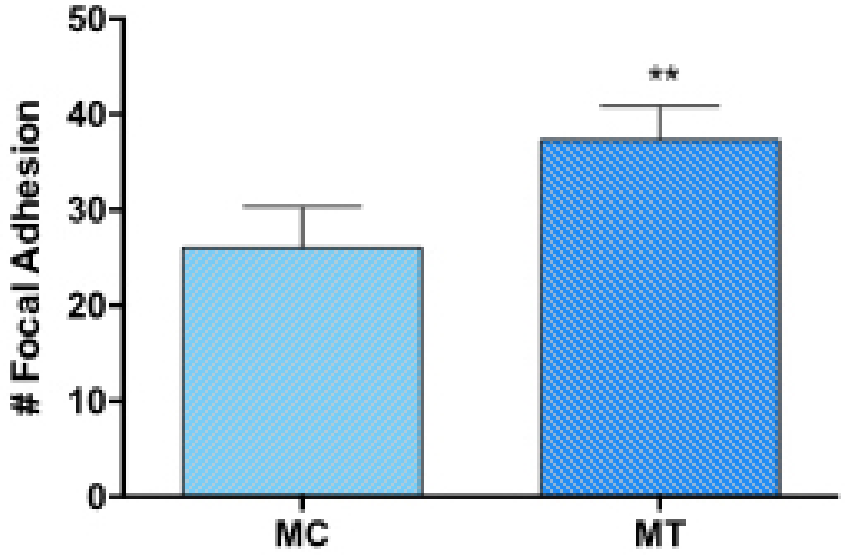

FIGURE 5.11: Histogram showing the average of focal adhesion detected for cell on machined surfaces. **=p<0.02.

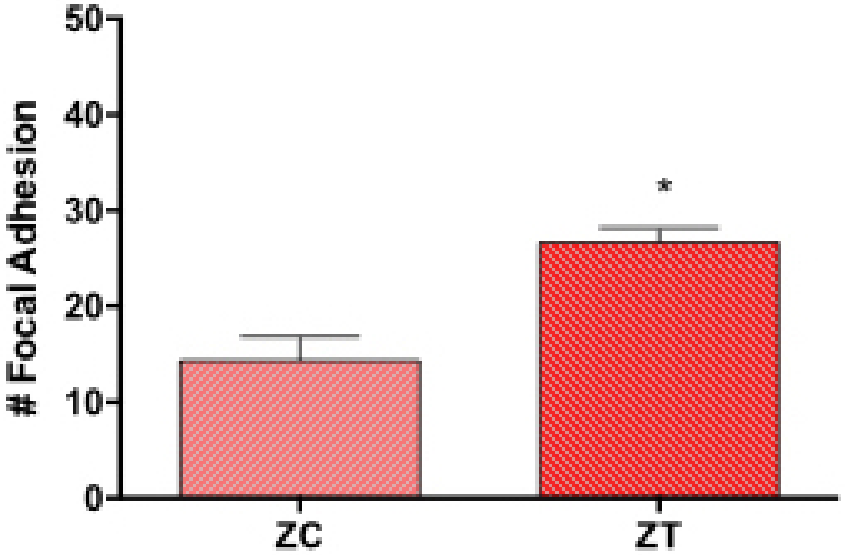

FIGURE 5.12: Histogram showing the average of focal adhesion detected for cell on ZirTi® surfaces. *=p<0.05.

5.4 Discussion

Nowadays, titanium dental implants are the most viable alternative for the replacement of missing teeth. Consequently, in the last few years, many efforts have been done in order to increase their performance by mimicking the innate characteristics of natural bone to promote osteoblast maturation [9], bone-to-implant contact [10] and clinical success [11, 12]. In this regard, it has been demonstrated that the characteristics of titanium surfaces, such as roughness, chemical composition and wettability profoundly affect the response of the surrounding tissues and a long-term outcome of the implant.

Titanium wettability (physically related to its energy) is one of the factors which mainly influence cell response to implants. Many studies have shown that hydrophilic surfaces tend to enhance cell adhesion and proliferation in the early stages of bone healing [13, 5]; and it seems that cell responses could be attributed to surface conditioning in the early stages of implant positioning, which is guided by the adsorption of circulating blood plasma proteins. Indeed, surface energy could alter protein adsorption at the interface by compromising the overall composition of the macromolecular film that covers the entire surface, thus altering cell behavior. In particular, it is noteworthy that hydrophilicity ameliorates titanium bioactivity by affecting (i) the amount of adsorbed proteins, (ii) the strength of their adsorption bonding and (iii) their conformation after the adsorption, which in the case of hydrophobic surfaces could lead to the masking of cell binding site [14].

In Chapter 4 we demonstrated that hyper-hydrophilicity enhanced all the cited parameters and improved surface selectivity for fibronectin

(fig.4.17 and 4.19), a protein involved in cell adhesion and proliferation [15]. To understand how these parameter affect cell behavior, we compared the responses of murine osteoblasts to rough or smooth normally hydrophilic or hyper hydrophilic surfaces, obtained with the previously descripted method.

Huang et al. have recently demonstrated that hydrophilicity is connected to an amelioration of cell adhesion to the surface [16]. In this work we showed that increased hydrophilicity on both machined and ZirTi® surfaces enhance osteoblasts adhesion. Twenty-four hours after seeding, the amount of adhering and viable cells was similar on the hyper hydrophilic surfaces and on their respective controls; however, investigating the rate of adhesion in the early moments after seeding, we showed that the rate of cell adhesion to the surface was significantly higher on the treated surfaces than on the controls for both machined and ZirTi® discs, and was faster for the machined hyper hydrophilic surfaces than for the ZirTi® one (fig.5.7 and 5.8).

Cell adhesion is a phenomenon strictly connected to cell morphology, an aspect which was thoroughly investigated through SEM-FIB analysis. Microphotographs reported in figure 5.9 show how surface hyper-hydrophilicity induced a close contact of cells to the underlying surface. The phenomenon was markedly evident for the ZirTi® surfaces (fig.5.9 G-L), where hyper hydrophilicity allowed a closer adhesion of cells, which appeared thinner and spread on the entire surface and which adhered preferentially to the titanium micro structure peaks, without gaps between the the cytoplasm and the substrate.

This observation was confirmed by focal adhesion immunostaining

in figure 5.10. Vinculin, a protein which mainly constitutes focal adhesions, was more highly expressed on the hyper hydrophilic surface than on the control, indicating close cell adhesion. Moreover, even though less evident for SEM-FIB analysis, we argue that ta similar phenomenon could be occurring on machined surfaces. In fact, although we could not appreciate significative differences in cell adhesion on the super hydrophilic surfaces by SEM-FIB (fig.5.9) probably because intrinsically flat surfaces did not induce any difference at this level, however we could observe an highly expression of focal adhesion after immunostaining (fig.5.10).

Bibliography

[1] Williams DF *The Williams dictionary of biomaterials.* The Liverpool University Press 1999.

[2] Branemark PI, Hansson BO, Adell R, Breine U, Lindstrom J, Hallen O, et al. *Osseointegrated implants in the treatment of the edentulous jaw. Experience from a 10-year period.* Scand J Plast Reconstr Surg Suppl 1977;16:1-132.

[3] Anselme K. *Osteoblast adhesion on biomaterials.* Biomaterials 2000;21:667-681.

[4] Eriksson C, Nygren H, Ohlson K. *Implantation of hydrophilic and hydrophobic titanium discs in rat tibia: cellular reactions on the surfaces during the first 3 weeks in bone.* Biomaterials 2004;25:4759-66.

[5] Bornstein MM, Jones AA, Wilson TG, Cochran DL. *Bone apposition around two different sandblasted and acid-etched titanium implant surfaces: a histomorphometric study in canine mandibles.* Clin Oral Implant Res. 2008;233–41.

[6] Rupp F, Gittens RA, Scheideler L, Marmur A, Boyan BD, Schwartz Z, Geins-Gerstorfer J. *A review on the gettability of dental implant surfaces I: Theoretical and experimental aspects.* Acta Biomater 2014;10(7):2894-906.

[7] Motta A (2005) *Dinamiche delle interazioni materiale-ambiente biologico.* In: Biomateriali - dagli impianti protesici alla medicina rigenerativa. Cigada et al. Vol.24, Patron editore, Bologna, pp.27-47 (ISBN 88-555-2836-X).

[8] Gittens RA, Scheideler L, Rupp F, Hyzy SL, Geis-Gerstorfer J, Schwartz Z, Boyan BD. *A review on the wettability of dental implant surfaces II: Biological and clinical aspects.* Acta Biomaterialia 10 (2014) 2907–2918.

[9] Gittens RA, Olivares-Navarrete R, Cheng A, Anderson DM, McLachlan T, Stephan I, et al. The Roles of *Titanium Surface Micro/Nanotopography and Wettability on the Differential Response of Human Osteoblast Lineage Cells.* Acta Biomater. 2013;9(4):6268–77.

[10] Kubo K, Tsukimura N, Iwasa F, Ueno T, Saruwatari L, Aita H, et al. *Biomaterials Cellular behavior on TiO 2 nanonodular structures in a micro-to-nanoscale hierarchy model.* Biomaterials. 2009;30(29):5319–29.

[11] Mendes VC, Moineddin R, Davies JE. *Discrete calcium phosphate nanocrystalline deposition enhances osteoconduction on titanium-based implant surfaces.* J Biomed Mater Res Part A. 2008.

[12] Lang NP, Salvi GE, Huynh-ba G, Donos N, Bosshardt DD, Bosshardt DD. *Early osseointegration to hydrophilic and hydrophobic implant surfaces in humans.* Clin Oral Implant Res. 2011;349–56.

[13] Ohlson K, Eriksson C. *Implantation of hydrophilic and hydrophobic titanium discs in rat tibia: cellular reactions on the surfaces during the first 3 weeks in bone.* Biomaterials. 2004;25:4759–66.

[14] Wilson CJ, Clegg RE, Leavesley DI, Pearcy MJ, et al. *Mediation of Biomaterial – Cell Interactions by Adsorbed Proteins: A Review.* 2005;11(1).

[15] Nuttelman CR, Mortisen DJ, Henry SM, Anseth KS. *Attachment of fibronectin to poly(vinyl alcohol) hydrogels promotes NIH3T3*

cell adhesion, proliferation, and migration. J Biomed Mater Res. 2001;57(2):217–23.

[16] Huang Q, Lin L, Yang Y, Hu R, Vogler EA, Lin C. *Biomaterials Role of trapped air in the formation of cell-and-protein micropatterns on superhydrophobic / superhydrophilic microtemplated surfaces.* Biomaterials. 2012;33(33):8213–20.

Chapter 6

Conclusions and future perspectives

6.1 Conclusions

The treatment we developed has proven effective in enhancing surfaces hydrophilicity, especially on ZirTi® surfaces. It is fundamental to underline that no major chemical nor morphological modifications occured on both ZirTi® and machined surfaces following the treatment, implying that the biological properties guaranteed by titanium dioxide biocompatibility and surface macro- and micro-topography are mantained.

Moreover, treated surfaces showed a marked selectivity for fibrinogen and fibronectin. Fibrinogen is a protein deeply involved in the inflammatory response cascade, so this peculiar property can positively influence the timing of tissue reparation and possibly, considering dental implant sites healing *in vivo*, accelerating osseointegration. Also fibronectin massive adsorption can be extremely useful in speeding-up osseointegration, being fibronectin one of the protein more involved in creating a functional osteoblasts-surface connection, enhancing osteoblast adhesion.

In vitro cellular experiments confirmed those hypothesis, showing that surfaces treated according to our method allowed a higher cell proliferation rate and a more functional cell adhesion, with osteoblast showing a flatter shape at SEM/FIB observations. Also cytofluorescence for vinculin confirmed these data, showing a greater number of focal adhesion on treated surfaces compared to non-treated ones.

Taken togheter, these data show the effectiveness of our treatment in enhancing hydrophilicity and consequently biological properties of titanium dental implant surfaces and open to the future possibility of using implants treated according to our method in clinical practice.

6.2 Future perspectives

In the next future, we will focus on preserving the obtained surface hydrophilicity over the time, trying to avoid the phenomenon of titanium biological aging. We hypotesize that hyper-hydrophilic titanium surfaces sealed in an environment free from organic contaminants could mantain their hydrophilicity level, becoming immune to biological aging.

We also believe that*in vivo* experiments could be fundamental to fully understand our titanium surface treatment potential in terms of osseointegration acceleration and hydrophilicity driven augmentation of bone to implant contact.